Non-Markovian dynamics of a system of two-level atoms coupled to a structured environment

H. Z. Shen,[1,2,*] Shuang Xu,[1] H. T. Cui,[3] and X. X. Yi[1,2,†]

[1]*Center for Quantum Sciences and School of Physics, Northeast Normal University, Changchun 130024, China*

[2]*Center for Advanced Optoelectronic Functional Materials Research, and Key Laboratory for UV Light-Emitting Materials and Technology of Ministry of Education, Northeast Normal University, Changchun 130024, China*

[3]*School of Physics and Optoelectronic Engineering, Ludong University, Yantai 264025, China*

(Received 1 July 2018; published 4 March 2019)

In this work, taking N noninteracting two-level atoms coupled to an anisotropic three-dimensional photonic crystal into account, we study exact non-Markovian dynamics of the atoms with the photonic crystal as an environment. We find that there exists a threshold number N_{CR} for the identical atoms, beyond which the system environment has a bound state regardless of how weak the system-environment coupling is. This means all identical atoms do not dissipate to the ground state. Further, when the whole system has no bound state, we find that the amplitude of collective excitation approaches a limit value $2/3$ as the number of atoms approaches to infinity. For nonidentical atoms with different transition frequencies, there exist N bound states at most that lead to N-wave mixing in the system dynamics. The present prediction is possible to observe in the recent circuit QED experiment, and the results suggest that coherence in a many-body system can be maintained in bound states by manipulating the environment.

DOI: 10.1103/PhysRevA.99.032101

I. INTRODUCTION

No quantum systems are fully isolated from their surroundings [1,2]. This unavoidable coupling would lead to decoherence and it is the main difficulty in quantum information processing. The dynamics of open system has attracted considerable attention in recent decades because it provides us with a model to understand numerous physical and chemical phenomena. Decoherence is the major obstacle that hinders the processing of quantum information in various physical implementations [3–5], and then the control of decoherence for open quantum systems is one of the challenging problems in the field of quantum information science [6,7].

Due to the strong memory effect of the environment, the non-Markovian decoherence dominates in nanoscale solid-state devices [8–10]. Besides, in the electron transport in semiconductors [11,12], the trapped atom coupled to an engineered reservoir [13], the dissipative light transport in photonic crystals [14], and in the structured environment [15–19], the non-Markovian decoherence appears possibly, because of where the correlation time of the environment is comparable with the time scale of the system.

Since coherence is the key resource in quantum information processing, it is natural to ask how to suppress the non-Markonvian decoherence. Is it different from that in a Markovian system? In fact, many schemes have been proposed for decoherence suppression including the non-Markovian coherent feedback control [20–22], the dynamical decoupling control [23–31], relaxation via dephasing [32], decoherence suppression induced by formation of bound states [33–54], bound states in the continuum [55–61], two-dimensional structured reservoirs [62–64], and three-dimensional state-dependent optical lattices [65] to mention a few.

The works of decoherence suppressions in non-Markovian systems are mainly based on the physics with a single two-level system subjected to the effects of structured environment [66–72], where the formation of system-environment bound state suppresses the decoherence induced by the feedback of environment on the system. However, system-environment bound state only exists when the coupling strength exceeds its threshold, which restricts the suppression of decoherence.

In this paper, taking a quantum system consisting of N noninteracting two-level atoms coupled to the structured environment into account, we show that the non-Markovian dissipation processes are effectively suppressed regardless of how weak the system-environment coupling is. We derive an analytical expression for the spectral density for the environment, and find that in the atoms there exists a threshold number beyond that the system-environment bound state always exists. This means all N identical atoms (same transition frequency) do not damp to their ground states. For nonidentical atoms with different transition frequencies, there exist at most N bound states, which leads to N-wave mixing of localized modes. It arises from the quantum interference of these bound states. Observations of the prediction in the recent circuit QED experiment can be realized in Refs. [36,73,74].

The remainder of this paper is organized as follows. In Sec. II, we introduce a model to describe N noninteracting two-level atoms subjected to the effects of an anisotropic three-dimensional photonic crystal (i.e., the environment), and derive coupled dynamical equations set in the single excitation space. In Sec. III, we study non-Markovian dynamics for N atoms. Section IV is devoted to derivations of bound states for the total system and a threshold of the number of atoms

*shenhz458@nenu.edu.cn

†yixx@nenu.edu.cn

is given. In Sec. V, we investigate non-Markovian dynamics for the atoms and find there exist N bound states at most, which leads to N-wave mixing of localized modes. Finally, we conclude in Sec. VI.

II. NON-MARKOVIAN DYNAMICS FOR N NONINTERACTING TWO-LEVEL ATOMS SYSTEM

The system under study is composed of N noninteracting two-level atoms coupled to a three-dimensional structured waveguide (Fig. 1). The waveguide is set along the x axis and supports a continuum of photonic modes. Then the dispersion relation near the band edge could be expressed as approximately in quadratical relations with the wave vector k [75]. The system is modeled as N two-level atoms system, where ground state $|g\rangle$ and excited state $|e\rangle$ of the jth atom are separated in frequency by ω_j ($j = 1, 2, \ldots, N$). Losses in the system are taken into account by coupling the N atoms to an infinite electromagnetic environment. The Hamiltonian of the total system can be expressed as

$$\hat{\mathcal{H}} = \hat{\mathcal{H}}_0 + \hat{\mathcal{H}}_I, \tag{1}$$

where

$$\hat{\mathcal{H}}_0 = \sum_{j=1}^{N} \hbar\omega_j \hat{\sigma}_j^+ \hat{\sigma}_j^- + \sum_k \hbar\Omega_k \hat{a}_k^\dagger \hat{a}_k \tag{2}$$

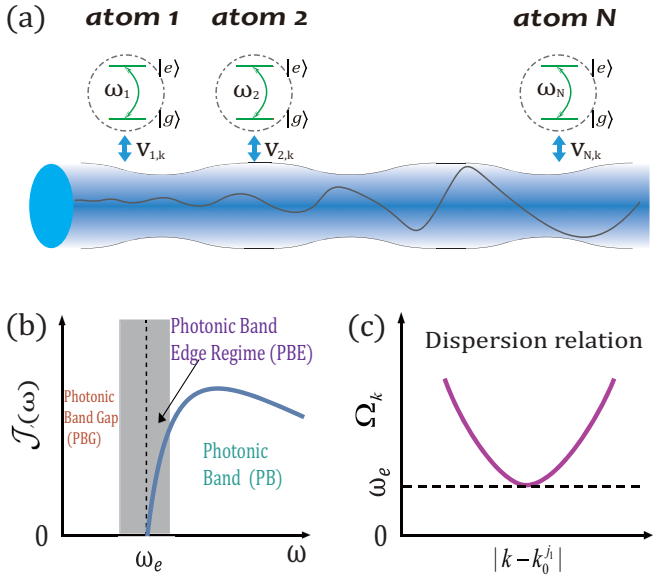

FIG. 1. Band structures of photonic crystals and localized photon modes. Setup: (a) N two-level atoms with transition frequencies ω_j coupled to a three-dimensional anisotropic photonic crystal with frequencies Ω_k, where the atoms can be tuned by the waveguide vacuum modes subjected to coupling coefficient $V_{j,k}$. It can be realized in recent circuit QED experiment [36,73,74]. (b) The spectral density $\mathcal{J}(\omega)$ in Eq. (14) of the two-level atoms coupled to photonic crystals, which can be derived in Appendix A. The spectrum is divided into three regimes: photonic band gap (PBG), the vicinity of the photonic band edge (PBE), and the photonic band (PB). (c) Dispersion relation (13) with photonic band edge ω_e for the system.

and

$$\hat{\mathcal{H}}_I = \sum_{j=1}^{N} \sum_k \hbar V_{j,k} \hat{\sigma}_j^- \hat{a}_k^\dagger + \hbar V_{j,k}^* \hat{a}_k \hat{\sigma}_j^+, \tag{3}$$

in which $\hat{\sigma}_j^+ (\hat{\sigma}_j^-)$ is the raising (lowering) operator of the jth atom with transition frequencies ω_j and $\hat{a}_k$ ($\hat{a}_k^\dagger$) is the annihilation (creation) operator of the kth field mode with frequencies Ω_k. Also, the strength of coupling between the jth atom and the kth field mode is represented by $V_{j,k}$. Hamiltonian (1) is analytically solvable due to the total excitation number $\hat{N} = \sum_{j,k} \hat{\sigma}_j^+ \hat{\sigma}_j^- + \hat{a}_k^\dagger \hat{a}_k$ being conserved. For simplicity, we initially prepare N atoms in a linear superposition of states with one exciton

$$|\psi(0)\rangle = \sum_{j=1}^{N} c_j \hat{\sigma}_j^+ |\mathrm{GS}\rangle, \tag{4}$$

where the normalized condition requires $\sum_{j=1}^{N} |c|_j^2 = 1$. $|\mathrm{GS}\rangle$ denotes the ground state of N atoms; simultaneously all the modes of the environment are all in the vacuum state, i.e., $|\mathrm{GS}\rangle = |g\rangle_1 \otimes |g\rangle_2 \otimes \cdots \otimes |g\rangle_N \otimes |0\rangle_1 \otimes |0\rangle_2 \otimes \cdots \otimes |0\rangle_\infty$. After time $t > 0$, the Schrödinger equation $i\hbar \frac{d}{dt}|\psi(t)\rangle = \hat{\mathcal{H}}|\psi(t)\rangle$ drives the initial state (4) to evolve to the following one:

$$|\psi(t)\rangle = \sum_{j=1}^{N} \mathcal{C}_j(t) \hat{\sigma}_j^+ |\mathrm{GS}\rangle + \sum_k \mathcal{R}_k(t) \hat{a}_k^+ |\mathrm{GS}\rangle, \tag{5}$$

where $\hat{\sigma}_j^+|\mathrm{GS}\rangle$ means that all of the atoms are in the ground state $|g\rangle$ except for the jth atom which is in the excited state $|e\rangle$ with the probability $|\mathcal{C}_j(t)|^2$. $\hat{a}_k^+|\mathrm{GS}\rangle$ denotes the environment only one excitation in the kth field mode with the probability $|\mathcal{R}_k(t)|^2$, but all other modes in environment are in the vacuum state. The probability amplitude for the jth atom is given by the following integro-differential equation [1]:

$$\frac{d\mathcal{C}_j(t)}{dt} = -i\omega_j \mathcal{C}_j(t) - \sum_{m=1}^{N} \int_0^t \mathcal{F}_{jm}(t-\tau)\mathcal{C}_m(\tau)d\tau, \tag{6}$$

where $j = 1, 2, \ldots, N$, and the correlation function

$$\mathcal{F}_{jm}(t-t') = \int d\omega\, \mathcal{J}_{jm}(\omega) e^{-i\omega(t-t')}, \tag{7}$$

with the spectral density of the structured environment given by

$$\mathcal{J}_{jm}(\omega) = \sum_k V_{j,k}^* V_{m,k} \delta(\omega - \Omega_k), \tag{8}$$

which characterizes all the back-actions between the atoms and photonic crystals and can be determined uniquely by the coupled strength $|V_{j,k}|^2$ between atoms and photonic crystals through the fluctuation dissipation relation (7). With the help of the probability amplitudes in Eq. (5) and the time-evolution equation (6), we can now express the reduced density matrix $\rho(t)$ of N atoms by tracing out the structured environment as

follows:

$$\rho(t)=\sum_{j=1}^{N}|\mathcal{C}_j(t)|^2\hat{\sigma}_j^+\hat{\sigma}_j^- +\sum_{m=1,n\neq m}^{N}\mathcal{C}_m(t)\mathcal{C}_n^*(t)\hat{\sigma}_m^+\hat{\sigma}_n^- +\left(1-\sum_{j=1}^{N}|\mathcal{C}_j(t)|^2\right)|\mathrm{GS}\rangle_{aa}\langle\mathrm{GS}|, \tag{9}$$

where $|\mathrm{GS}\rangle_a$ denotes the ground state of N atoms, i.e., $|\mathrm{GS}\rangle_a=|g\rangle_1\otimes|g\rangle_2\otimes\cdots\otimes|g\rangle_N$.

In the following several sections, based on the coupled dynamical equation set given by Eq. (6), we will discuss the non-Markovian dynamics for the identical (Secs. III and IV) and nonidentical atoms with different transition frequencies (Sec. V) in the anisotropic three-dimensional photonic crystal environment, respectively.

III. NON-MARKOVIAN DYNAMICS FOR N IDENTICAL ATOMS

A. Analytical expression of probability amplitude

In this section, we consider the N atoms are all identical (same transition frequency), i.e., $\omega_j\equiv\omega_c$. Via considering explicitly N atoms coupled dissipatively to a bosonic environment, we show that the bound states can be formed by modulating the number of atoms N. This implies that the non-Markovian dynamics can be controlled through engineering the bound state via manipulating the number of atoms of the quantum system. To grasp qualitatively the physics behind the threshold in the non-Markovian effect, we first solve Eq. (6) by Laplace transformation [76–79] that yields

$$\mathcal{C}_j(s)=\frac{\mathcal{C}_j(0)-\sum_{m=1}^{N}\mathcal{F}_{jm}(s)\mathcal{C}_m(s)}{s+i\omega_c}, \tag{10}$$

where

$$\mathcal{F}_{jm}(s)=\int\frac{\mathcal{J}_{jm}(\omega)}{s+i\omega}d\omega. \tag{11}$$

In the anisotropic three-dimensional photonic crystal [80], the coupling coefficient $V_{j,k}$ takes

$$V_{j,k}=(\omega_j d_j/\hbar)\sqrt{\hbar(2\varepsilon_0\Omega_k V)}\vec{e}_k\cdot\vec{u}_j, \tag{12}$$

where k represents both the momentum and the polarization of the modes. d_j and $\vec{u}_j$ are the magnitude and unit vector of the atomic dipole moment of the transition. V is the quantization volume. $\vec{e}_k$ are the transverse unit vectors for the environment modes and ε_0 denotes the vacuum dielectric constant. If a three-dimensional anisotropic photonic crystal has an allowed point-group symmetry, the dispersion relation near the band edge could be expressed approximately with [75]

$$\Omega_k=\omega_e+A\left|\vec{k}-\vec{k}_0^{j_1}\right|^2, \tag{13}$$

where ω_e is the cutoff frequency of the band edge. $\vec{k}_0^{j_1}$ are the finite collections of symmetry related points, which are associated with the band edge. The parameter A is the model-dependent constant. Using the dispersion relation (13), and converting the mode sum over transverse plane waves into an integral and performing the integral, we analytically derive spectral density of the structured environment $\mathcal{J}_{jm}(\omega)=\gamma_{jm}^{3/2}\sqrt{\omega-\omega_e}\phi(\omega-\omega_e)/(\pi\omega)$, where $\gamma_{jm}^{3/2}=(\omega_j d_j)(\omega_m d_m)\sum_{j_1}\sin^2(\theta_{j_1})/(4\pi\varepsilon_0\hbar A^{3/2})$ with θ_{j_1} being the angle between the dipole vector of the atom and the j_1th $k_0^{j_1}$. $\phi(\omega-\omega_e)$ is an unit step function, i.e., $\phi(\omega-\omega_e)=1$ for $\omega\geqslant\omega_e$; otherwise, $\phi(\omega-\omega_e)=0$. For simplicity, and without loss of generality, below we assume $\gamma_{jm}\equiv\gamma$ since we can make the atomic dipole moments of two transitions parallel to each other and appropriately adjust the magnitude for atomic dipole moment d_j, d_m and atomic transition frequency ω_j, ω_m. Therefore, the spectral density of the structured environment is reduced to

$$\mathcal{J}(\omega)=\frac{\gamma^{3/2}}{\pi}\frac{\sqrt{\omega-\omega_e}}{\omega}\phi(\omega-\omega_e), \tag{14}$$

where γ denotes the effective coupling constant between atomic system and structured environment. More details of Eq. (14) can be found in Appendix A.

Substituting Eq. (14) into Eq. (11), we obtain frequency-domain correlation function

$$\mathcal{F}(s)=\frac{-i\gamma^{3/2}}{\sqrt{\omega_e}+\sqrt{-is+\omega_e}}, \tag{15}$$

where the phase angle of s is defined by $-\pi<\arg(s)<\pi$; the phase angle of $\sqrt{-is+\omega_e}$ in $\mathcal{F}(s)$ is defined by $-\frac{\pi}{2}<\arg\sqrt{-is+\omega_e}<\frac{\pi}{2}$. The excited-state amplitudes $\mathcal{C}_j(t)$ of jth atom can then be obtained by means of an inverse Laplace transformation

$$\mathcal{C}_j(t)=\frac{1}{2\pi i}\int_{\sigma-i\infty}^{\sigma+i\infty}\mathcal{C}_j(s)e^{st}ds, \tag{16}$$

where $\mathcal{C}_j(s)$ is given by Eq. (B2). The real number σ is conditionally chosen so that $s=\sigma$ lies to the right of all the singularities (poles and branch points) of functions $\mathcal{C}_j(s)$. With the help of complex function integration and the residue theorem, we can obtain the expression of the probability amplitude for the jth atom:

$$\mathcal{C}_j(t)=\mathcal{I}_j(t)+\frac{1}{N}\mathcal{C}(t), \tag{17}$$

where the collective probability amplitude

$$\mathcal{C}(t)=\mathcal{C}(0)\left\{\sum_m\frac{e^{x_m^{(1)}t}}{\mathcal{G}'\left(x_m^{(1)}\right)}+\sum_n\frac{e^{x_n^{(2)}t}}{\mathcal{L}'\left(x_n^{(2)}\right)}+\frac{1}{2\pi i}\times\int_0^\infty dy\,\mu(-y-i\omega_e)e^{-yt-i\omega_e t}\right\} \tag{18}$$

describes the global motion for N identical atoms, where $\mathcal{C}(0)=\sum_{j=1}^{N}\mathcal{C}_j(0)$. The contribution from the initial population is given by

$$\mathcal{I}_j(t)=e^{-i\omega_c t}\left[\mathcal{C}_j(0)-\frac{\mathcal{C}(0)}{N}\right], \tag{19}$$

where $\mathcal{G}(s)$ and $\mathcal{L}(s)$ can be found in Eq. (B4) and Eq. (B6) in Appendix B. $\mu(s)=\mathcal{L}^{-1}(s)-\mathcal{G}^{-1}(s)$, where $\mathcal{G}'(s)$ and $\mathcal{L}'(s)$ are derivatives of functions $\mathcal{G}(s)$ and $\mathcal{L}(s)$, respectively. $x_m^{(1)}$ and $x_n^{(2)}$ are the roots of $\mathcal{G}(s)=0$ and $\mathcal{L}(s)=0$, respectively.

The dynamics can be calculated from the sum of different contributions shown in Fig. 2(a). Contour of integration for

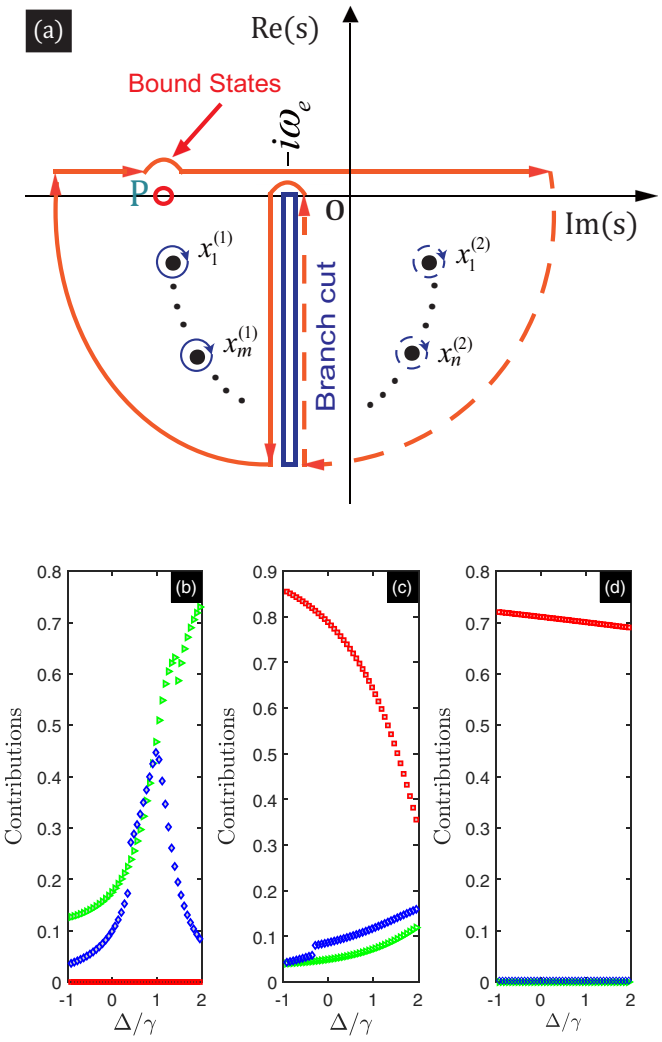

FIG. 2. Contour of integration for anisotropic three-dimensional photonic crystal environment taking one detour at the band edges $s = -i\omega_e$ to avoid the branch cuts. (b) Contributions to the collective dynamics at steady state for a situation with $\omega_e = \gamma$ as a function of the detuning Δ: bound state [corresponding to the first term of Eq. (18), red square], nonlocalized mode [corresponding to the second term of Eq. (18), green-right-deltoid], nonexponential damp [corresponding to the third term of Eq. (18), blue *diamond*]. The parameters chosen are $N = 1$ (b), $N = 3$ (c), and $N = 100$ (d).

photonic crystal environment takes one detour at the band edges $s = -i\mathcal{E}_{\rm BS}$ to avoid the branch cuts. The second term $\mathcal{C}(t)$ of Eq. (17) denotes the collective exciton dynamics, which is different from those in Refs. [81–88], where no bound states are formed. This can be seen from Hamiltonian (1). If we define the collective annihilation and creation operators $\hat{S}^- = \sum_{j=1}^{N} \hat{\sigma}_j^-$ and $\hat{S}^+ = (\hat{S}^-)^\dagger$, respectively, Hamiltonian (1) reduces to Jaynes-Cummings model ($V_{j,k} \to V_k$)

$$\hat{\mathcal{H}}_{\rm eff} = \hbar\omega_c \hat{S}_z + \sum_k \hbar\Omega_k \hat{a}_k^\dagger \hat{a}_k + \sum_k \hbar V_k \hat{S}^- \hat{a}_k^\dagger + \hbar V_k^* \hat{a}_k \hat{S}^+. \tag{20}$$

In order to illuminate the collective effect of the number of atoms on the photonic crystal system, and avoid confusion for the influence of initial states on the evolution, we assume that the initial population is $c_j \equiv N^{-1/2}$, which leads to $\mathcal{I}_j(t) \equiv 0$ given by Eq. (19). In this case, the time-evolution state (5) can be written as

$$|\psi_{\rm eff}(t)\rangle = \frac{\mathcal{C}(t)}{N}\hat{S}^+|{\rm GS}\rangle + \sum_k R_k(t)\hat{a}_k^+|{\rm GS}\rangle. \tag{21}$$

From Hamiltonian (20) and whole time-evolution state (21), we can see that they are independent of any specific atoms. Therefore, $\mathcal{C}(t)$ can be seen as a collective motion to the jth atom, so that in this system the total atoms present the same dynamical behavior-collective motion.

The first term in Eq. (17) denotes the contributions of the initial atoms population on the system dynamics. The first term in Eq. (18) corresponds to localized modes with $s = -i\mathcal{E}_n$ ($\mathcal{E}_n$ are real numbers, which correspond to the energy spectrum of the whole system), which appears as a consequence of the so-called photon bound states [see red *square* lines in Fig. 2(b)]. The localized modes exist if and only if the environmental spectral density has band gaps located at the pure imaginary zeros with $\mathcal{G}(-i\mathcal{E}_n) = 0$ [see point P in Fig. 2(a)]. These localized modes do not decay, which give dissipationless non-Markovian dynamics. The nonlocalized mode contains two parts. One is the second term in Eq. (18) [see green-right-deltoid lines in Fig. 2(b)], which is the oscillating damping process due to the complex roots in $\mathcal{L}(s) = 0$ in the regime of [$\mathrm{Re}(s) < 0$ and $\mathrm{Im}(s) < -\omega_e$]. The other is the integral part, i.e., the nonexponential parts will oscillate rapidly in time [see blue *diamond* lines in Fig. 2(b)]. This rapidly oscillating damping originates from the terms containing $e^{-i\omega_e t}$ in Eq. (18). Therefore, the nonlocalized mode parts in Eq. (18) are the contribution of the allowed bands, which usually generate exponential decays.

We show that the probability amplitudes in Eq. (17) from the Lebesgue-Riemann lemma [89] in the long-time regime ($t \to \infty$) reach

$$\mathcal{C}_j(t \to \infty) = \mathcal{I}_j(t) + \frac{\mathcal{C}(0)}{N}\sum_m \frac{e^{x_m^{(1)}t}}{\mathcal{G}'\left(x_m^{(1)}\right)}, \tag{22}$$

whose probability represents a periodic function that changes over time, which does not fully dissipate to the structured environment. Equation (17) is of vital importance in studying the system dynamics, which is the key element to time evolution of the jth atom. So far, we have presented a derivation for the non-Markovian dynamics of N identical atoms. Since Eq. (17) only depends on the initial state (4), in the next section we only study the collective dynamics to the system.

B. Collective dynamics

Since in this model all atoms are indistinguishable, they behave identically. Independent of the number of atoms N, there are thus just N independent components of the steady-state density matrix within the single-excitation subspace. In fact, the localized mode and the nonexponential damping indicates the existence of the non-Markovian memory dynamics. As one can see in Fig. 3, where the number of atoms $N = 1$, when the atom frequency is tuned far away from the

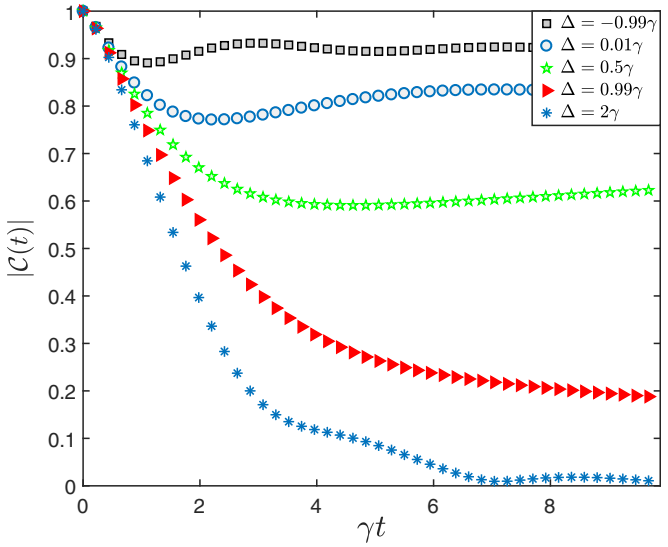

FIG. 3. Time evolution of the population for one atom coupled to a three-dimensional anisotropic photonic crystal with different detuning $\Delta = \omega_c - \omega_e$. The parameters chosen are $\omega_e = \gamma$, $N = 1$.

PBG ($\Delta = 2\gamma$), the collective amplitude of atoms is rapidly damped. When the atom frequency lies in the vicinity of the PBE, the nonexponential non-Markovian damping dominates the photon dynamics. When the atom frequency is tuned deeply inside the PBG, the atom has almost no damping, and thus photons can be confined in the defect of the photonic crystal. In fact, the photon dissipative non-Markovian dynamics produces the same results with regard to atomic population trapping (inhibition of spontaneous emissions) and atom-photon bound states in the vicinity of the photonic band gap, obtained by John and others [33,35,80] when an atom is placed in the defect. Figure 4 shows the numerical result of long-time $|\mathcal{C}(t \to \infty)|$ in the different detuning Δ. One can check that $|\mathcal{C}(t \to \infty)|$ just represents the time evolution

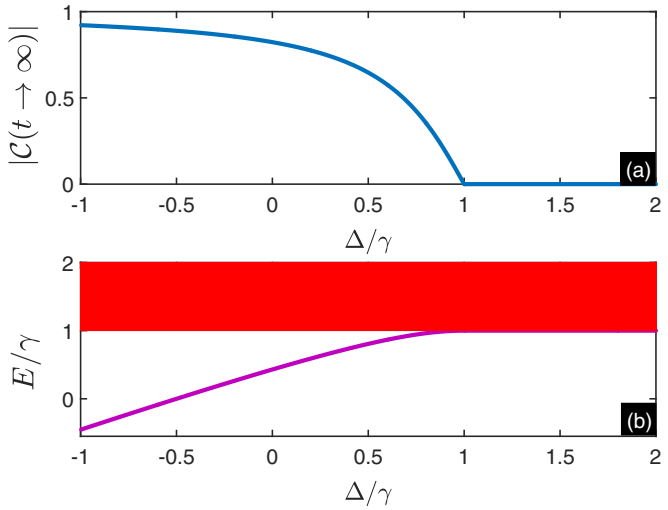

FIG. 4. (a) Steady state $|\mathcal{C}(t \to \infty)|$ in different detuning Δ. (b) Energy spectrum of the atom-environment system, where the red regime denotes the energy band. Here $\omega_e = \gamma$, $N = 1$.

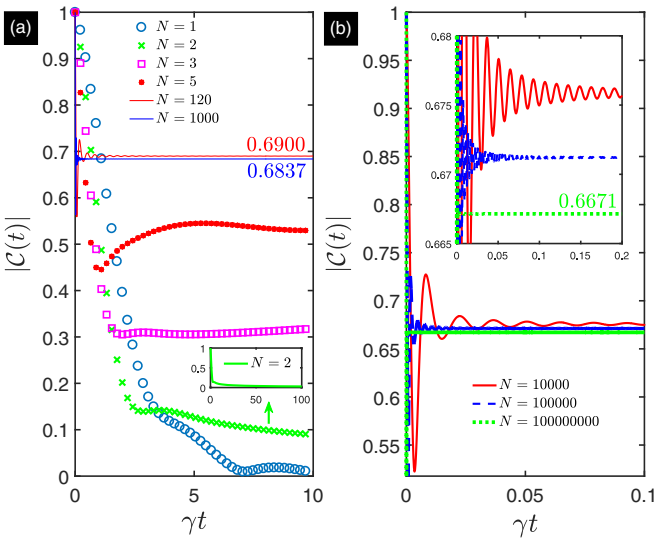

FIG. 5. Time evolution of the population for N identical atoms coupled to a three-dimensional anisotropic photonic crystal with the number of atoms in fixed atom-photonic crystal parameters, where $\Delta = 2\gamma$ and $\omega_e = \gamma$. With these parameters, we can obtain the threshold $N_{\mathrm{CR}} = 3$ obtained from Eq. (33). From the figure, we find the collective probability amplitude in the excited state increases with the increase of the number of atoms N, which originates from the formation of atoms-photonic crystal with the increase of the number of atoms ($N \geqslant 3$). From the figure, we find the excitation population reaches the steady value 0.6671 when the number of atoms is $N = 100\,000\,000$.

of one atom. It is interesting to find that, for $\Delta/\gamma < 1$, the atom can be partially stabilized in its excited state even in the presence of the dissipative environment.

Interestingly, for the number of atoms $N > 1$ with fixed atom-photonic crystal environment parameters, we set $\Delta = 2\gamma$. It has been shown that there is no bound state in this system for $N = 1$, which leads to the collective amplitude damping to the ground states. However, when we increase the number of atoms to very large values, e.g., $N = 3, 5, 120, 1000$, the values of $|\mathcal{C}(t)|$ tend to stabilize [see Fig. 5(a)]. As the number of atoms increases further, e.g., $N = 100\,000\,000$, the population no longer changes and is fixed to 0.6671 [see green-dotted line in Fig. 5(b)]. To gain more insight into the N-atoms-manipulated non-Markovian dynamics shown in Figs. 3 and 5, we below give the physical origin behind the dynamics.

IV. FORMATION OF BOUND STATES FOR THE TOTAL SYSTEM

A. Formation of bound states for N-atoms environment

We show that the non-Markovian dynamics of an open system connects closely with the energy-spectrum signatures of the whole system (system plus environment). Therefore, the investigation of the energy spectrum may provide us insight to understand its dynamics. In a single atom coupled with the environment, it is known that the whole system (system plus its environment) can form a bound state [36–38], which is actually a stationary state with a vanishing decay rate during

the time evolution. If such a bound state is formed, then it will lead to a dissipationless dynamics. In this section, we point out that the system-environment bound states are easily controlled by tuning the number of atoms and atomic transition frequency. Since the total exciton of the whole system $\hat{N}$ is conserved, the Hilbert space splits into independent subspaces with definite $\hat{N}$. For our zero temperature non-Markovian environment, only the subspaces with $\hat{N} = 0$ and 1 are involved in the dynamics. Besides the trivial eigenstate $|\psi_0\rangle = |\mathrm{GS}\rangle$ with $\mathcal{E}_0 = 0$ for the $\hat{N} = 0$ subspace, we can obtain the eigenstate of the $\hat{N} = 1$ subspace as $|\psi_{\mathrm{BS}}\rangle = \sum_{j=1}^{N} \mathcal{D}_j \hat{\sigma}_j^+ |\mathrm{GS}\rangle + \sum_k \mathcal{S}_k \hat{a}_k^+ |\mathrm{GS}\rangle$ satisfies eigenequation

$$\hat{\mathcal{H}}|\psi_{\mathrm{BS}}\rangle = \mathcal{E}|\psi_{\mathrm{BS}}\rangle. \tag{23}$$

After simple calculations, we obtain the closed equation about eigenvalues as follows:

$$\mathcal{E}\mathcal{D}_j = \omega_j \mathcal{D}_j + \sum_{m=1}^{N} \sum_k \frac{V_{j,k}^* V_{m,k} \mathcal{D}_m}{\mathcal{E} - \Omega_k}. \tag{24}$$

It is very difficult to solve Eq. (24) due to the j dependence of the coupling strength $V_{j,k}$. In order to study the properties of the bound state for the whole system, in this section we assume that $V_{j,k}$ does not depend on subscript j for the jth atom. In this case, the condition for the jth atom probability amplitude $\mathcal{D}_j$ having nontrivial solutions is that the determinant of the coefficient matrix of Eq. (24)

$$\mathcal{A} = \begin{bmatrix} \omega_1 + \mathcal{Z}_1 - \mathcal{E}, \mathcal{Z}_1, \cdots \mathcal{Z}_1 \\ \mathcal{Z}_1, \omega_2 + \mathcal{Z}_1 - \mathcal{E}, \cdots \mathcal{Z}_1 \\ \vdots \quad \vdots \qquad\qquad \vdots \\ \mathcal{Z}_1, \mathcal{Z}_1, \cdots \omega_N + \mathcal{Z}_1 - \mathcal{E} \end{bmatrix}_{N\times N} \tag{25}$$

is equal to zero [i.e., $\det(\mathcal{A}) = 0$ for $N \geqslant 2$]. This will lead to the identity $\mathcal{Z}_1 \equiv \mathcal{Z}_1(\mathcal{E}) = \mathcal{Z}_2(\mathcal{E})$, where

$$\mathcal{Z}_1(\mathcal{E}) = \sum_k \frac{|V_k|^2}{\mathcal{E} - \Omega_k} \tag{26}$$

and

$$\mathcal{Z}_2(\mathcal{E}) = \frac{\prod_{m=1}^{N}(\mathcal{E} - \omega_m)}{\chi_N} \tag{27}$$

where,

$$\chi_N = \sum_{k=1}^{N} (-1)^{N-k} k \mathcal{E}^{k-1} \sum_{m_1<m_2<\cdots m} \underbrace{\omega_{m_1}\omega_{m_2}\cdots\omega_m}_{m=N-k}. \tag{28}$$

In this case, by imposing Eq. (26) being equal to Eq. (27), we can obtain N solutions for the bound states at most (also see the discussion of Sec. V).

Especially, for N identical atoms, i.e., $\omega_j \equiv \omega_c$ [43], Eq. (24) will lead to a compact form as

$$\mathcal{B}(\mathcal{E}) \equiv \omega_c - N \int_{\omega_e}^{\infty} \frac{\mathcal{J}(\omega)d\omega}{\omega - \mathcal{E}} = \mathcal{E}, \tag{29}$$

where $\mathcal{J}(\omega)$ is given by Eq. (14). Solution of Eq. (29) highly depends on the particular choice of the spectral density of the structured environment and the number of atoms. It is clear that the existence of a bound state in the spectrum of Eq. (23) requires that Eq. (29) must have at least a real solution in the energy range: $\mathcal{E} < \omega_e$. In general, existence of bound states in the spectrum of the total Hamiltonian depends on the fact that Eq. (29) must satisfy the condition $\mathcal{B}(\omega_e) < \omega_e$, i.e.,

$$\omega_c - N \int_{\omega_e}^{\infty} \frac{\mathcal{J}(\omega)d\omega}{\omega - \omega_e} < \omega_e. \tag{30}$$

Otherwise, the bound state is not formed. To simplify the discussion, with the spectral density $\mathcal{J}(\omega)$ given by Eq. (14), we define parameter η as

$$\eta \equiv \int_{\omega_e}^{\infty} \frac{\mathcal{J}(\omega)d\omega}{\omega - \omega_e} = \frac{\gamma^{3/2}}{\sqrt{\omega_e}}. \tag{31}$$

Then Eq. (30) can be reduced to

$$\Delta < N\eta, \tag{32}$$

where $\Delta = \omega_c - \omega_e$. Especially, for $N = 1$, the whole system forms a bound state if $\Delta < \eta$ (see $\Delta/\gamma < 1$ for formation of the bound state with $\omega_e = \gamma$ in Figs. 3 and 4).

For $N > 1$ and $\Delta/\eta > 1$, inequality in Eq. (32) is broken if $1 \leqslant N < [[\Delta/\eta + 1]]$ ($[[x]]$ denotes the integer party of x). In this case, the whole system does not form a bound state, which leads to the excited-state probability amplitude $\mathcal{C}(t)$ decaying to zero in the long-time limit. However, there exists a bound state in the system no matter how large the ratio Δ/η for $N \geqslant [[\Delta/\eta + 1]]$, where Eq. (32) is satisfied. Therefore, the threshold for the number of atoms

$$N_{\mathrm{CR}} = [\![\Delta/\eta + 1]\!] \equiv \left[\!\left[\frac{\Delta\sqrt{\omega_e}}{\gamma^{3/2}} + 1 \right]\!\right] \tag{33}$$

can be regarded as a critical number of atoms. With the definition above, we show that the condition $N \geqslant N_{\mathrm{CR}}$ guarantees the whole system to form a bound state, which leads to strong non-Markovian dynamics in any coupling regime.

Keeping the system parameters fixed, the greater the number of atoms (regardless of the weakness of coupling), the stronger the non-Markovianity. An interesting fact arises that as $\Delta > \eta$ (i.e., when all the N atoms are all in large detuning regimes from the environment), the whole system can still form bound states if $N \geqslant N_{\mathrm{CR}} = 3$ in Fig. 5. Moreover, the weaker the N atoms coupled to the environment, the greater the number N of atoms required to guarantee the onset of non-Markovian dynamics. For $N = 2 < N_{\mathrm{CR}}$, the two atoms are not enough to resist the decay of the environment, and finally all damp to the ground states (see x line in Fig. 5). For $N = 3 \geqslant N_{\mathrm{CR}}$, the effective coupling strength of the three atoms exceeds the critical coupling strength, allowing the system environment to form a bound state. In the long-time limit, the collective amplitude has a certain probability in

the excited state:

$$|\mathcal{C}(t\to\infty)| = \frac{1}{1+\frac{\gamma^{3/2}N}{2\sqrt{\omega_e-\mathcal{E}_{\rm BS}}(\sqrt{\omega_e}+\sqrt{\omega_e-\mathcal{E}_{\rm BS}})^2}}, \tag{34}$$

where the $\mathcal{E}_{\rm BS}$ denotes the bound states given by Eq. (B4) via the replacement $s=-i\mathcal{E}_{\rm BS}$, i.e., $\mathcal{G}(-i\mathcal{E}_{\rm BS})=-i\mathcal{E}_{\rm BS}+i\omega_c+N\mathcal{F}(-i\mathcal{E}_{\rm BS})=0$. In principle, the system's non-Markovian dynamics can always be obtained by just adding a sufficiently large number of atoms as long as Δ/η is finite. As the number of atoms increases further, the excited state of the atom reaches a limit value. Taking the limit to atoms number $N\to\infty$, we analytically verify

$$|\mathcal{C}(t\to\infty)|_{N\to\infty} = \tfrac{2}{3} \approx 0.667, \tag{35}$$

which is consistent with the result 0.6671 obtained by taking the number of atoms $N = 100\,000\,000$ [see the green-dotted line in Fig. 5(b)]. Our results are different from those obtained from Refs. [90–93]. In Refs. [90,91], the authors discussed a case where full emission occurs for one atom whereas population trapping occurs with two atoms, but our result is generalized to unlimited number of atoms. References [92,93] showed the superradiance emission exists near a photonic band edge in a structured reservoir. In our case, from Eq. (B1), if we define effective coupling strength $\gamma_{\rm eff}=N\gamma$, the collective amplitude $\mathcal{C}(t)$ reduces to the case of single atom coupled with the environment, but the coupling strength γ is replaced by the effective coupling strength $\gamma_{\rm eff}$. In this case, $\gamma_{\rm eff}$ is increased indefinitely with fixed γ by adding the number of atoms in nonzero detuning $\Delta\neq 0$. When the number of atoms N exceeds this threshold $N_{\rm CR}$, the effective coupling strength $\gamma_{\rm eff}$ exceeds the critical coupled strength, which means that the system-environment bound state always exists regardless of the weakness of system-environment coupling strength. This means N all-identical atoms do not dissipate to the ground state of N identical atoms. Physically, the back action of the environment experienced by each atom is enhanced by the action of other atoms, as the number of atoms increases indefinitely. This enhanced feedback from the non-Markovian environment to the system makes the population of the collective atom reach a stable value. Based on Eqs. (17) and (35), we obtain the steady probability amplitude for the jth atom:

$$\mathcal{C}_j(t\to\infty) = e^{-i\omega_c t}\left[C_j(0)-\frac{1}{N}\right]+\frac{2\mathcal{C}(0)}{3N}e^{-i\mathcal{E}_{\rm BS}t}. \tag{36}$$

Therefore, in the long-time limit, each atom exhibits the behavior of periodic oscillations, which originates from the quantum interference of bound-state and atom resonance state. This means that there are two mechanisms of information backflow at work: (1) the excitation dissipations induced by the coupling between the atom and photonic crystal and (2) the formation of bound states between the atoms and the environments. The competition between the two effects determines the finite maximum value of populations.

B. Concurrence

We now investigate time evolution of entanglement for two atoms. In this case, the structure of the bound state (23) can be reduced to the Bell-like state

$$|\psi_{\rm BS}\rangle_{12} = \sqrt{2}|\Phi_{\rm BS}\rangle\otimes|{\rm GS}\rangle+\hat{\varphi}|{\rm GS}\rangle, \tag{37}$$

where $\hat{\varphi}=\sum_k \mathcal{S}_k\hat{a}_k^+$, and $|\Phi_{\rm BS}\rangle$ is the (maximally entangled) Bell state:

$$|\Phi_{\rm BS}\rangle = \frac{1}{\sqrt{2}}(|eg\rangle+|ge\rangle)_{12}. \tag{38}$$

This is a key feature which enables entanglement generation by atom-photon interaction.

In the long-time limit, the atomic density matrix $\rho(\infty)$ approaches

$$\rho(\infty) = 2\mathcal{D}^2|\Phi_{\rm BS}\rangle\langle\Phi_{\rm BS}|+(1-2\mathcal{D}^2)|gg\rangle_{12}\langle gg|, \tag{39}$$

which denotes the dominate role of the $\rho(\infty)$ formed in the long-time steady state. On the contrary, if no bound states formed, then $\rho(\infty)=|gg\rangle_{12}\langle gg|$. The results verify analytically from the point of view of the dynamics the validity of our expectation that the reduced state of the formed bound state is of our decoherent system. The preserved steady-state population matches well with ${\rm Tr}[\rho(\infty)\sum_{j=1,2}\hat{\sigma}_j^+\hat{\sigma}_j^-]=2\mathcal{D}^2$ calculated analytically from Eq. (34), which verifies unambiguously that the initial state evolves exclusively to the steady state $\rho(\infty)$ obtained in Eq. (39).

In Fig. 6, we plot the evolution of the entanglement between the two atoms. The entanglement is quantified by concurrence [94], which for the state is $Concurrence = 2|\mathcal{C}_1(t)\mathcal{C}_2(t)|$. We find that the parameter regimes in unformed bound state $N<N_{\rm CR}$, where a vanish entanglement occurs and match exactly well with the blue-*circle* line in Fig. 5. With the further decrease of detuning so that the parameter satisfies the bound-state condition, e.g., $\Delta=\gamma$, a finite concurrence is obtained (blue-$*$ line). The concurrence approaches the analytical value $2|\mathcal{D}|^2$, which is just the concurrence calculated from the steady state (39). It demonstrates

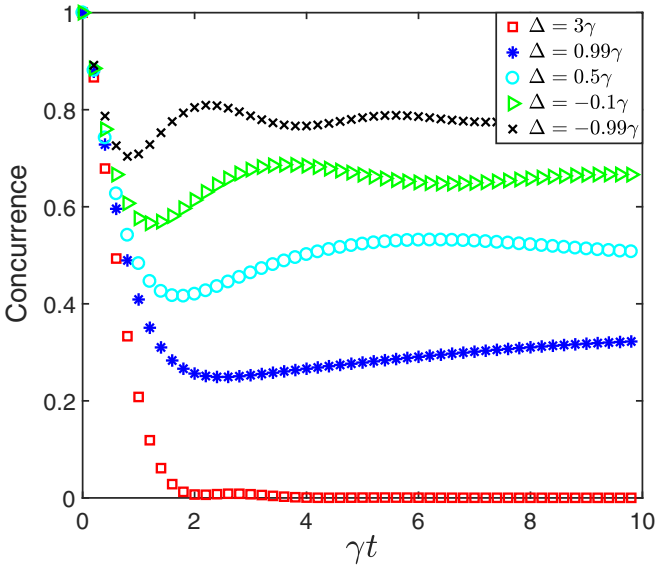

FIG. 6. Behavior of the concurrence of the two atoms as a function of the time t with different detunings. The parameters chosen are $\omega_e=\gamma$, $N=2$.

well the distinguished role played by the formed bound-state dynamics and steady-state behavior.

C. Emission spectra near the anisotropic three-dimensional photonic crystal band edge

In order to illuminate the effect of the number of atoms on the photonic crystal system, we calculate the emission spectrum of the system. In order to achieve this goal, we assume that the initial population takes $c_j \equiv N^{-1/2}$, which leads to $\mathcal{I}_j(t) \equiv 0$ and $\mathcal{C}(0) = \sqrt{N}$. In this case, the whole state (21) does not depend on $\mathcal{I}_j(t)$. Therefore, in this system the total atoms present the same dynamical behavior-collective motion. The emission spectrum of the system $S(\omega)$ is defined by the Fourier transformation of the correlation function $\langle \hat{S}^+(t)\hat{S}^-(0)\rangle$ through the Wiener-Khintchine relation as [95–97]

$$S(\omega) = \int_{-\infty}^{\infty} e^{-i\omega t'} \langle \hat{S}^+(t')\hat{S}^-(0)\rangle dt' + \text{c.c.}, \tag{40}$$

where c.c. stands for the complex conjugate of the leading term. If we used the initial condition $\mathcal{C}(0) = 1$ and assumed the ensemble average was stationary, which meant independent of time, this spectrum can be written as

$$S(\omega) = 2\,\text{Re}\left\{\int_{-\infty}^{\infty} e^{-i\omega t'}\mathcal{C}(t')dt'\right\} = 2\,\text{Re}\{\mathcal{C}(s=-i\omega)\}. \tag{41}$$

Taking the real part of $\mathcal{C}(s=-i\omega)$, we analytically get the emission spectrum

$$S(\omega) = \begin{cases} 0, & \omega \leqslant \omega_e, \\ \frac{2\gamma^{3/2}N\omega\sqrt{\omega-\omega_e}}{\gamma^3N^2(\omega-\omega_e)+[(\Delta-\omega+\omega_e)\omega-\gamma^{3/2}N\sqrt{\omega_e}]^2}, & \omega > \omega_e. \end{cases} \tag{42}$$

The emission spectra behavior of the anisotropic photonic crystal system could also be studied through the emission spectrum shown in Fig. 7. This figure is plotted according to Eq. (42), where the definition of emission spectrum is based on the Wiener-Khintchine relation [95–97]. This spectrum exhibits no emission of radiation in the photonic band gap ($N \geqslant N_{\text{CR}} = [[\Delta/\gamma + 1]]$) and the allowed band ($N < N_{\text{CR}} = [[\Delta/\gamma + 1]]$) (see *circle* lines in Fig. 7) because of the absence and abundance of photon spectrum density in these two regions. For the large atoms $N \geqslant N_{\text{CR}}$ region [see Figs. 7(c) and 7(d)], this spectrum changes from the allowed band to the photonic band gap, which are in good agreement with those given by time-evolution dynamics for identical atoms in Fig. 5.

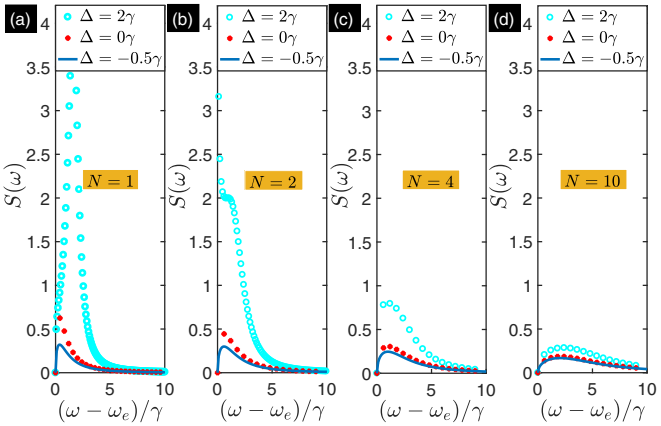

FIG. 7. Emission spectra near an anisotropic band edge of a photonic crystal for several atomic detuning frequencies from the band edge in units of γ. From Eq. (33), with $\omega_e = \gamma$, we find $N_{\text{CR}} = [[\Delta/\gamma + 1]]$. Therefore, systems with positive atomic detuning frequencies have atomic frequencies lying within the allowed band, while those with negative ones $\Delta < 0$ inside the PBG under $N = 1$. We find, with the increase of the number of atoms, positive atomic detuning frequencies $\Delta > 0$ all enter the PBG.

V. NONIDENTICAL ATOMS WITH DIFFERENT TRANSITION FREQUENCIES

In the previous section, we systematically studied the exact non-Markovian dynamics of N identical atoms. Equation (17) provides general solutions of the non-Markovian dissipative dynamics for the system consisting of N identical atoms in three-dimensional photonic crystal structures. It shows that the atoms dynamics in photonic crystal always contains two parts: a localized photon mode (the second term) where there is at most one bound state and nonlocalized mode (the other terms except the second term) photon damping. The corresponding frequency-energy spectrum always exists within the PBG. This nonlocalized mode damping is a short-time non-Markovian memory effect, and it will become an exponential decay in the PB region. Below we will point out that there exist two (three) bound states at most for two (three) nonidentical atoms with different transition frequencies ($\omega_1 \neq \omega_2 \neq \omega_3$), which leads to very interesting dynamical behaviors fully different from the case of N identical atoms. For two nonidentical atoms, we analytically obtain probability amplitudes

$$\begin{aligned}\mathcal{C}_1(t) &= \sum_m \frac{h_1(s_m^{(1)})e^{s_m^{(1)}t}}{\mathcal{G}_2'(s_m^{(1)})} + \sum_n \frac{h_3(s_n^{(2)})e^{s_n^{(2)}t}}{\mathcal{L}_2'(s_n^{(2)})} \\ &\quad + \frac{1}{2\pi i}\int_0^{\infty} dy\,\mu_1(-y - i\omega_e)e^{-yt-i\omega_e t}, \\ \mathcal{C}_2(t) &= \sum_m \frac{h_2(s_m^{(3)})e^{s_m^{(3)}t}}{\mathcal{G}_2'(s_m^{(3)})} + \sum_n \frac{h_4(s_n^{(4)})e^{s_n^{(4)}t}}{\mathcal{L}_2'(s_n^{(4)})} \\ &\quad + \frac{1}{2\pi i}\int_0^{\infty} dy\,\mu_2(-y - i\omega_e)e^{-yt-i\omega_e t},\end{aligned} \tag{43}$$

where the relevant coefficients can be found in Appendix C.

For three atoms, we obtain probability amplitudes

$$\begin{aligned}\mathcal{C}_1(t) &= \sum_m \frac{g_1(s_m^{(1)})e^{s_m^{(1)}t}}{\mathcal{G}_3'(s_m^{(1)})} + \sum_n \frac{g_4(s_n^{(2)})e^{s_n^{(2)}t}}{\mathcal{L}_3'(s_n^{(2)})} \\ &\quad + \frac{1}{2\pi i}\int_0^{\infty} dy\,\nu_1(-y - i\omega_e)e^{-yt-i\omega_e t},\end{aligned}$$

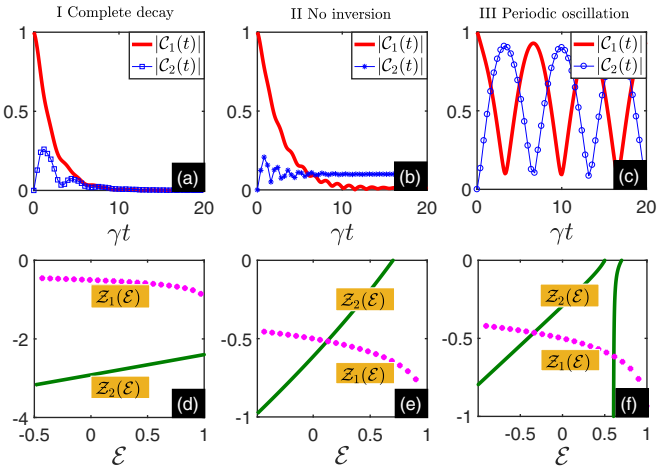

FIG. 8. Time evolution of the population for two atoms with different transition frequencies ($\omega_1 \neq \omega_2$). The red-solid and blue-dotted lines denote the population $|\mathcal{C}_j(t)|$ for atom 1 and atom 2, respectively. The initial state takes $\mathcal{C}_1(0) = 1$, $\mathcal{C}_2(0) = 0$. This figure corresponds to complete decay, no inversion, and periodic oscillation, respectively. The parameters chosen are $\omega_1 = 5\gamma$, $\omega_2 = 7\gamma$ for (a) and (d), $\omega_1 = 5\gamma$, $\omega_2 = 0.7\gamma$ for (b) and (e), and $\omega_1 = 0.5\gamma$, $\omega_2 = 0.7\gamma$ for (c) and (f). The energy spectrum $\mathcal{E}$ is scaled in units of γ. The points of intersection of the $\mathcal{Z}_1(\mathcal{E})$ and $\mathcal{Z}_2(\mathcal{E})$ denote the bound states in the system.

$$\mathcal{C}_2(t) = \sum_m \frac{g_2(s_m^{(3)})e^{s_m^{(3)}t}}{\mathcal{G}_3'(s_m^{(3)})} + \sum_n \frac{g_5(s_n^{(4)})e^{s_n^{(4)}t}}{\mathcal{L}_3'(s_n^{(4)})} + \frac{1}{2\pi i}\int_0^\infty dy\, \nu_2(-y - i\omega_e)e^{-yt - i\omega_e t},$$

$$\mathcal{C}_3(t) = \sum_m \frac{g_3(s_m^{(3)})e^{s_m^{(5)}t}}{\mathcal{G}_3'(s_m^{(3)})} + \sum_n \frac{g_6(s_n^{(4)})e^{s_n^{(6)}t}}{\mathcal{L}_3'(s_n^{(4)})} + \frac{1}{2\pi i}\int_0^\infty dy\, \nu_3(-y - i\omega_e)e^{-yt - i\omega_e t}, \quad (44)$$

where relevant coefficients can also be found in Appendix C.

For two and three nonidentical atoms with different transition frequencies, we summarize four independent regions as follows.

(i) Complete decay of atoms. We discuss in details the features of four different regimes for two atoms in Fig. 8 and three atoms in Fig. 9. First, in the PB region, where the localized mode vanishes due to there being no real root in PB, the exciton dynamics undergoes a full dissipation process [see Figs. 8(a) and 9(a)]. It can be approximately characterized as a nonlocalized mode, which contains two parts. One is the second term in Eqs. (43) and (44), which is the oscillating damping process due to the complex roots in $\mathcal{L}_{2(3)}(s) = 0$ in the regime of [$\mathrm{Re}(s) < 0$ and $\mathrm{Im}(s) < -\omega_e$]. The other is the integral part, i.e., the nonexponential parts will oscillate rapidly in time. This rapidly oscillating damping originates from the terms containing $e^{i\omega_e t}$ in Eqs. (43) and (44).

(ii) No inversion of population. The nonlocalized mode parts will rapidly approach zero within the PBG according to the Lebesgue-Riemann lemma. In this case there is only one real energy spectrum; therefore, the population Eqs. (43) and

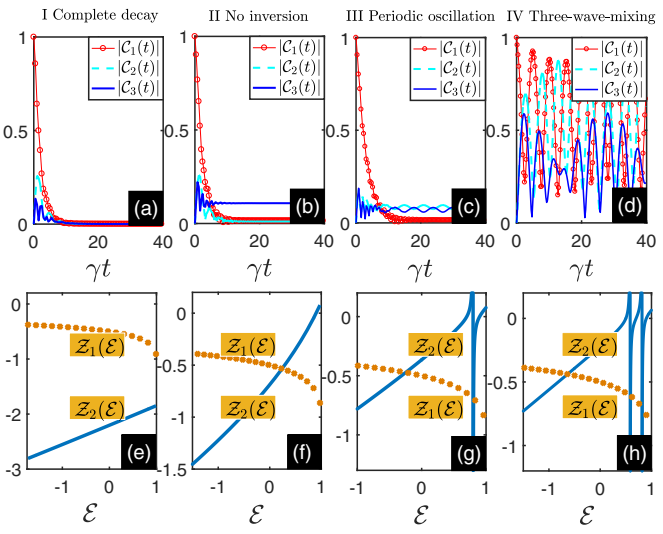

FIG. 9. Time evolution of the population for two nonidentical atoms ($\omega_1 \neq \omega_2 \neq \omega_3$). The red-solid, green-dashed, and blue-dashed-dotted lines denote the population $|\mathcal{C}_j(t)|$ for atom 1, atom 2, and atom 3, respectively. The initial state takes $\mathcal{C}_1(0) = 1$, $\mathcal{C}_2(0) = 1 = 0$, $\mathcal{C}_3(0) = 0$. This case corresponds to complete decay, no inversion, periodic oscillation, and three-wave mixing, respectively. The parameters chosen are $\omega_1 = 5\gamma$, $\omega_2 = 7\gamma$, $\omega_3 = 9\gamma$ for (a) and (e), $\omega_1 = 5\gamma$, $\omega_2 = 7\gamma$, $\omega_3 = 0.9\gamma$ for (b) and (f), $\omega_1 = 5\gamma$, $\omega_2 = 0.7\gamma$, $\omega_3 = 0.9\gamma$ for (c) and (g), and $\omega_1 = 0.5\gamma$, $\omega_2 = 0.7\gamma$, $\omega_3 = 0.9\gamma$ for (d) and (h). The energy spectrum $\mathcal{E}$ is scaled in units of γ. The points of intersection of the $\mathcal{Z}_1(\mathcal{E})$ and $\mathcal{Z}_2(\mathcal{E})$ denote the bound states in the system.

(44) can be obtained [see Figs. 8(b) and 9(b)] after a long time:

$$|\mathcal{C}_j(t \to \infty)| = \frac{h_j(-i\mathcal{E}_{\mathrm{BS2}})}{\mathcal{G}_2'(-i\mathcal{E}_{\mathrm{BS2}})}, \quad (45)$$

where $\mathcal{E}_{\mathrm{BS2}}$ is a pure imaginary root of $\mathcal{G}_2(s = -i\mathcal{E}_{\mathrm{BS2}})$ [see Fig. 8(e)]. For three atoms

$$|\mathcal{C}_j(t \to \infty)| = \frac{g_j(-i\mathcal{E}_{\mathrm{BS3}})}{\mathcal{G}_3'(-i\mathcal{E}_{\mathrm{BS3}})}, \quad (46)$$

where $\mathcal{E}_{\mathrm{BS3}}$ is a pure imaginary root of $\mathcal{G}_3(s = -i\mathcal{E}_{\mathrm{BS3}})$ [see Fig. 9(f)]. We find that population holds a nonzero steady value after a long time. This is also understandable based on the fact that the bound state, as a stationary state of the whole system, has a vanishing decay rate and the coherence contained in it would be preserved during the time evolution.

(iii) Periodic oscillation of atoms with different transition frequencies. Interestingly, in this case, the quantum interference effects between the two localized modes after large time t lead to periodic oscillation behaviors of the dynamics. The amplitudes of periodic oscillations do not decrease in time. From Eqs. (43) and (44), we obtain the populations for two atoms in the long-time regime for two atoms,

$$|\mathcal{C}_1(t \to \infty)| = \varepsilon_1^2\varepsilon_2^2 + \varepsilon_1\varepsilon_2 \cos[(\mathcal{E}_{\mathrm{BS1}} - \mathcal{E}_{\mathrm{BS2}})t], \quad (47)$$

and for three atoms,

$$|\mathcal{C}_1(t \to \infty)| = \varepsilon_3^2\varepsilon_4^2 + \varepsilon_3\varepsilon_4 \cos[(\mathcal{E}_{\mathrm{BS3}} - \mathcal{E}_{\mathrm{BS4}})t], \quad (48)$$

whose periodic is $T = 2\pi/(\mathcal{E}_{\mathrm{BS1}} - \mathcal{E}_{\mathrm{BS2}})$ or $2\pi/(\mathcal{E}_{\mathrm{BS3}} - \mathcal{E}_{\mathrm{BS4}})$. Here $\mathcal{E}_{\mathrm{BS1}}$ and $\mathcal{E}_{\mathrm{BS2}}$ is a pure imaginary root of

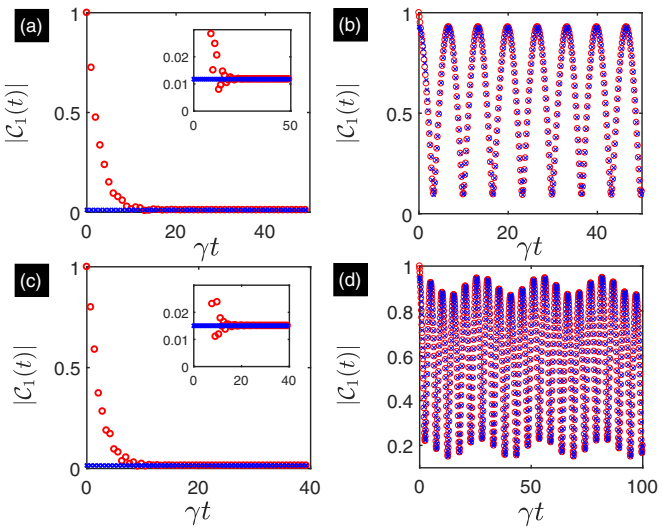

FIG. 10. Comparison of $|\mathcal{C}_1(t)|$ calculated by solving Eq. (43) [(a) and (b)] (red circles) and Eq. (44) [(c) and (d)] (red circles) and by evaluating the steady solution (49) (blue $\times$) in two atoms [(a) versus (45) and (b) versus (47)], and three atoms [(c) versus (46) and (d) versus (49)]. Other parameters are $\omega_1 = 5\gamma, \omega_2 = 7\gamma$ for (a), $\omega_1 = 0.5\gamma,\ \omega_2 = 0.7\gamma$ for (b), $\omega_1 = 5\gamma,\ \omega_2 = 7\gamma, \omega_3 = 9\gamma$ for (c), and $\omega_1 = 0.5\gamma,\ \omega_2 = 0.7\gamma,\ \omega_3 = 0.9\gamma$ for (d).

$\mathcal{G}_2(s = -i\mathcal{E}_{\rm BS})$ [see Fig. 8(f)] and $\mathcal{E}_{\rm BS3}$ and $\mathcal{E}_{\rm BS4}$ is a pure imaginary root of $\mathcal{G}_3(s = -i\mathcal{E}_{\rm BS})$ [see Fig. 9(g)]; these coefficients take $\varepsilon_1 = \frac{h_1(-i\mathcal{E}_2)}{\mathcal{G}_2'(-i\mathcal{E}_2)}$, $\varepsilon_2 = \frac{h_1(-i\mathcal{E}_3)}{\mathcal{G}_2'(-i\mathcal{E}_3)}$, $\varepsilon_3 = \frac{g_1(-i\mathcal{E}_2)}{\mathcal{G}_2'(-i\mathcal{E}_2)}$, $\varepsilon_4 = \frac{g_1(-i\mathcal{E}_3)}{\mathcal{G}_2'(-i\mathcal{E}_3)}$. The dynamics reaches periodic oscillation behaviors. In other words, the nonlocalized mode will approach zero after some time due to the localized exciton dynamics. The short-time dynamics is given by Figs. 8(c) and 9(c). The changes from complete decoherence to decoherence suppression and then to periodic oscillation results from the existence of bound states in the model itself (see Figs. 8 and 9).

(iv) Three-wave mixing of three atoms with different transition frequencies. In this subsection, we give the analytical population for the first atom

$$\sum_{j=1}^{3} |A_j^2| + 2 \sum_{m<n=1}^{3} |A_n A_m^*| \cos[(\mathcal{E}_{{\rm BS}m} - \mathcal{E}_{{\rm BS}n})t + \varphi_m], \quad (49)$$

where $A_j = \frac{g_1(-i\mathcal{E}_{{\rm BS}j})}{\mathcal{G}_3'(-i\mathcal{E}_{{\rm BS}j})}$ and $\mathcal{E}_{{\rm BS}j}$ $(j = 1, 2, 3)$ are three pure imaginary roots of $\mathcal{G}_3(s = -i\mathcal{E}_{{\rm BS}j})$. The conditions of bound states in three atoms at most exist as three bound states, which leads to three-wave mixing mediating the conversion of a photon with different frequencies. This can be exhibited in Fig. 9(d) [Fig. 9(h) shows that there are three bound states in this case].

Figure 10 depicts the results of $|\mathcal{C}_1(t)|$. The results are obtained by solving Eq. (43) [(a) and (b)] (red circles) and Eq. (44) [(c) and (d)] (red circles), by evaluating the steady solution (49) (blue $\times$) in two atoms [(a) versus Eq. (45) and (b) versus Eq. (47)], and three atoms [(c) versus Eq. (46) and (d) versus Eq. (49)]. Comparing these results, we find that the numerical result, except the small difference in short-time regime, coincides exactly with the steady result in the long-time limit. When only two bound states are formed for two atoms, $|\mathcal{C}_1(t)|$ shows the perfect oscillation with the period $T = 2\pi/(\mathcal{E}_{\rm BS1} - \mathcal{E}_{\rm BS2})$ [see Fig. 10(b)]. When three bound states are formed, $|\mathcal{C}_1(t)|$ shows the three-wave mixing oscillation with multiple frequencies determined jointly by $\mathcal{E}_{\rm BS1}$, $\mathcal{E}_{\rm BS2}$, and $\mathcal{E}_{\rm BS3}$ due to the interference between the three bound states [see Fig. 10(d)]. The comparison validates unambiguously the bound-states mechanism in governing the atoms with different transition frequencies induced by the anisotropic three-dimensional photonic crystal environment.

VI. CONCLUSIONS

In summary, we have investigated non-Markovian dynamics for N noninteracting two-level systems coupled to an anisotropic three-dimensional photonic crystal. We show that the dissipation of N atoms can always be effectively suppressed as long as the number of atoms exceeds the threshold, beyond which the system-environment exists the bound state. This is quite different from the situation with single atom. For atoms with different transition frequencies, there exist N bound states at most, which leads to N-wave mixing of N localized modes. This discovery is attributed to the formation of a bound state between each atom and its quantum environment. The result provides us with an active way to realize the control of the quantum many-body system by engineering the environment [36,73,74].

Our results are observable in the circuit QED platform [36,73,74], where the bound state has been observed already. Note that current studies might be extendable to a nonrotating wave system [98], as well as other spectral densities (e.g., the Ohmic spectrum) [99]; hence it is interesting for the community of quantum physics.

ACKNOWLEDGMENTS

This work is supported by the National Natural Science Foundation of China (NSFC) under Grants No. 11534002, No. 11775048, and No. 11705025, and Science Foundation of the Education Department of Jilin Province during the 13th Five-Year Plan Period under Grant No. JJKH20190262KJ.

APPENDIX A: SPECTRAL DENSITY OF PHOTONIC CRYSTAL ENVIRONMENTS

With Eqs. (8) and (12), we can calculate spectral density of the structured environment as follows:

$$\begin{aligned}\mathcal{J}_{jm}(\omega) &= \sum_k V_{j,k}^* V_{m,k} \delta(\omega - \Omega_k) \\ &= \frac{\varepsilon_{jm}}{2\varepsilon_0 \hbar V} \sum_k \frac{(\vec{e}_k \cdot \vec{u}_j)(\vec{e}_k \cdot \vec{u}_m)}{\Omega_k} \delta(\omega - \Omega_k) \\ &= \frac{\varepsilon_{jm}}{2\varepsilon_0 \hbar V} \sum_k \frac{1 - (\vec{k} \cdot \vec{u}_j)(\vec{k} \cdot \vec{u}_m)/k^2}{\Omega_k} \delta(\omega - \Omega_k) \\ &= \frac{\varepsilon_{jm}}{16\pi^3 \varepsilon_0 \hbar} \int \frac{[1 - (\vec{k} \cdot \vec{u}_j)(\vec{k} \cdot \vec{u}_m)/k^2] d^3\vec{k}}{\Omega_k} \delta(\omega - \Omega_k), \end{aligned} \quad (A1)$$

where $\varepsilon_{jm} = (\omega_j d_j)(\omega_m d_m)$, and we have replaced the sum by an integral via $\sum_k \to V(2\pi)^{-3}\int d^3\vec{k}$ and $(\vec{e}_k\cdot\vec{u}_j)(\vec{e}_k\cdot\vec{u}_m) = 1-(\vec{k}\cdot\vec{u}_j)(\vec{k}\cdot\vec{u}_m)/k^2$. Near the band edge, the dispersion relation may be expressed approximately by $\Omega_k = \omega_e + A|\vec{k}-\vec{k}_0^{j_1}|^2$. We only consider that the atomic dipole moments are parallel [100]; it was shown that a system can emulate to a large degree a system with parallel dipole moments, and systems with parallel dipoles can be realized in Ref. [101]. Therefore, the angle between the dipole vector of the jth atom and the j_1th $\vec{k}_0^{j_1}$ is all θ_{j_1}. The angle between the dipole and $\vec{k}$ near $\vec{k}_0^{j_1}$ is replaced approximately by θ_{j_1}. Then Eq. (A1) is reduced to

$$\begin{aligned}\mathcal{J}_{jm}(\omega) &= \frac{\varepsilon_{jm}}{16\pi^3\varepsilon_0\hbar}\left(\sum_{j_1}\sin^2\theta_{j_1}\right)\int\frac{d^3\vec{q}}{(\omega_c+A|\vec{q}|^2)}\\ &\quad\times\delta(\omega-\omega_c-A|\vec{q}|^2)\\ &= \frac{\varepsilon_{jm}}{4\pi^2\varepsilon_0\hbar}\left(\sum_{j_1}\sin^2\theta_{j_1}\right)\int_0^\infty\frac{q^2dq}{(\omega_c+Aq^2)}\\ &\quad\times\delta(\omega-\omega_c-Aq^2).\end{aligned}\tag{A2}$$

In the continuum limit, $\mathcal{J}_{jm}(\omega)$ can be written as

$$\begin{aligned}\mathcal{J}_{jm}(\omega) &= \frac{\varepsilon_{jm}}{4\pi^2\varepsilon_0\hbar}\left(\sum_{j_1}\sin^2\theta_{j_1}\right)\int_0^\infty\frac{q^2dq}{(\omega_c+Aq^2)}\\ &\quad\times\delta(\omega-\omega_e-Aq^2).\end{aligned}\tag{A3}$$

According to the properties of the Dirac delta function, we have

$$\mathcal{J}_{jm}(\omega) = \frac{\gamma_{jm}^{3/2}A^{3/2}}{\pi}\sum_n\frac{q_n^2(\omega)}{\omega}\left|\frac{A\,dq^2}{dq}\right|^{-1}_{q=q_n(\omega)},\tag{A4}$$

where $\gamma_{jm}^{3/2} = \varepsilon_{jm}\sum_{j_1}\sin^2(\theta_{j_1})/(4\pi\varepsilon_0\hbar A^{3/2})$, and the corresponding wave numbers $q_n(\omega)$ are determined by

$$\omega = \omega_e + Aq^2(\omega).$$

Substituting the above results into Eq. (A4), we can obtain the spectral density (14) for the anisotropic three-dimensional photonic crystal environment.

APPENDIX B: CALCULATION OF THE COLLECTIVE AMPLITUDES $\mathcal{C}(t)$

The amplitude $\mathcal{C}(t) = \sum_{j=1}^N \mathcal{C}_j(t)$ can be obtained by means of the inverse Laplace transform,

$$\begin{aligned}\mathcal{C}(t) &= \frac{1}{2\pi i}\int_{\sigma-i\infty}^{\sigma+i\infty}\mathcal{C}(s)e^{st}ds\\ &= \frac{1}{2\pi i}\int_{\sigma-i\infty}^{\sigma+i\infty}ds\,e^{st}\frac{\mathcal{C}(0)}{s+i\omega_c+N\mathcal{F}(s)},\end{aligned}\tag{B1}$$

where $\mathcal{C}(s)$ is given by

$$\mathcal{C}(s) = \frac{\mathcal{C}(0)}{s+i\omega_c+N\mathcal{F}(s)}.\tag{B2}$$

With the integration contours as shown in red-solid line of Fig. 2(a), we have

$$\begin{aligned}\mathcal{C}(t) = \sum_m\frac{\mathcal{C}(0)e^{x_m^{(1)}t}}{\mathcal{G}'(x_m^{(1)})} - \frac{\mathcal{C}(0)}{2\pi i}\Bigg\{\int_{-i\omega_e-\infty}^{-i\omega_e+0}+\int_{-i\infty+0}^{-i\infty+0}ds\,e^{st}\\ \times\frac{C(0)}{s+i\omega_c+NF(s)}\Bigg\},\end{aligned}\tag{B3}$$

where the function

$$\mathcal{G}(s) = s+i\omega_c+N\mathcal{F}(s),\tag{B4}$$

where $x_m^{(1)}$ is the root of the equation $\mathcal{G}(s)=0$ in the region [$\mathrm{Re}(s)>0$ or $\mathrm{Im}(s)>-\omega_e$], the real number σ, and the real number $s=\sigma$ lies to the right of all the singularities $x_m^{(1)}$. The last term can be calculated with the integration contours in red-dashed line as shown Fig. 2(a):

$$\begin{aligned}&\frac{1}{2\pi i}\int_{-i\omega_e+0}^{-i\infty+0}ds\,e^{st}\frac{\mathcal{C}(0)}{s+i\omega_c+N\mathcal{F}(s)}\\ &\quad=\frac{1}{2\pi i}\int_{-i\omega_e}^{-i\infty}ds\,e^{st}\frac{\mathcal{C}(0)}{s+i\omega_c+N\mathcal{F}_1(s)}\\ &\quad=-\sum_n\frac{\mathcal{C}(0)e^{x_n^{(2)}t}}{\mathcal{L}'(x_n^{(2)})}-\frac{\mathcal{C}(0)}{2\pi i}\\ &\qquad\times\left[\int_{-i\omega_e-\infty}^{-i\omega_e+0}ds\,e^{st}\frac{\mathcal{C}(0)}{s+i\omega_c+N\mathcal{F}_1(s)}\right],\end{aligned}\tag{B5}$$

where

$$\mathcal{L}(s) = s+i\omega_c+N\mathcal{F}_1(s),\quad \mathcal{F}_1(s) = \frac{-i\gamma^{3/2}}{\sqrt{\omega_e}-i\sqrt{is-\omega_e}},\tag{B6}$$

where $x_n^{(2)}$ is the root of the equation $\mathcal{L}(s)=0$ in the region [$\mathrm{Re}(s)<0$ and $\mathrm{Im}(s)<-\omega_e$]. From Eqs. (B1), (B3), and (B5), we can obtain the amplitudes (18) by setting $s=-y-i\omega_e$.

APPENDIX C: RELEVANT COEFFICIENTS FOR TWO ATOMS AND THREE ATOMS

For nonidentical atoms with different transition frequencies, enjoying the similar methods as one atom above, we can derive the exact non-Markovian dynamics (43) and (44) for two and three atoms, respectively. Below we list these coefficients. For the case of two atoms, they are

$$\begin{aligned}\mathcal{G}_2(s) &= s^2+\mathcal{F}(s)(2s+i\omega_1+i\omega_2)+is\omega_1+is\omega_2-\omega_1\omega_2,\\ \mathcal{L}_2(s) &= s^2+\mathcal{F}_1(s)(2s+i\omega_1+i\omega_2)+is\omega_1+is\omega_2-\omega_1\omega_2,\end{aligned}$$

$$\begin{aligned}h_1(s) &= \mathcal{C}_1(0)[\mathcal{F}(s)+s+i\omega_2]-\mathcal{F}(s)\mathcal{C}_2(0),\\ h_2(s) &= \mathcal{F}(s)[\mathcal{C}_2(0)-\mathcal{C}_1(0)]+\mathcal{C}_2(0)(s+i\omega_1),\\ h_3(s) &= \mathcal{C}_1(0)[\mathcal{F}_1(s)+s+i\omega_2]-\mathcal{F}_1(s)\mathcal{C}_2(0),\\ h_4(s) &= \mathcal{F}_1(s)[\mathcal{C}_2(0)-\mathcal{C}_1(0)]+\mathcal{C}_2(0)(s+i\omega_1),\end{aligned}$$

$$\begin{aligned}\mathcal{F}(s) &= -i\gamma^{3/2}/(\sqrt{\omega_e}+\sqrt{-is+\omega_e}),\\ \mathcal{F}_1(s) &= -i\gamma^{3/2}/(\sqrt{\omega_e}-i\sqrt{is-\omega_e}),\end{aligned}$$

$$\mu_1(s) = h_3(s)/\mathcal{L}_2(s) - h_1(s)/\mathcal{G}_2(s),$$
$$\mu_2(s) = h_4(s)/\mathcal{L}_2(s) - h_2(s)/\mathcal{G}_2(s).$$

While for three atoms, we list the coefficients as follows:

$$\begin{aligned}
\mathcal{G}_3(s) &= (s+i\omega_1)(s+i\omega_2)(s+i\omega_3) + \mathcal{F}(s) \\
&\quad \times [3s^2 - \omega_1\omega_2 - \omega_1\omega_3 - \omega_2\omega_3 \\
&\quad + 2is(\omega_1+\omega_2+\omega_3)], \\
\mathcal{L}_3(s) &= (s+i\omega_1)(s+i\omega_2)(s+i\omega_3) + \mathcal{F}_1(s) \\
&\quad \times [3s^2 - \omega_1\omega_2 - \omega_1\omega_3 - \omega_2\omega_3 \\
&\quad + 2is(\omega_1+\omega_2+\omega_3)], \\
g_1(s) &= \mathcal{C}_1(0)(s+i\omega_2)(s+i\omega_3) - \mathcal{F}(s) \\
&\quad \times [\mathcal{C}_3(0)(s+i\omega_2) + \mathcal{C}_2(0)(s+i\omega_3) - \mathcal{C}_1(0) \\
&\quad \times (2s + i(\omega_2+\omega_3))], \\
g_2(s) &= \mathcal{C}_2(0)(s+i\omega_1)(s+i\omega_3) - \mathcal{F}(s)[\mathcal{C}_3(0)(s+i\omega_1) \\
&\quad + \mathcal{C}_1(0)(s+i\omega_3) - \mathcal{C}_2(0)(2s + i(\omega_1+\omega_3))], \\
g_3(s) &= \mathcal{C}_3(0)(s+i\omega_1)(s+i\omega_2) - \mathcal{F}(s)[\mathcal{C}_2(0)(s+i\omega_1) \\
&\quad + \mathcal{C}_1(0)(s+i\omega_2) - \mathcal{C}_3(0)(2s + i(\omega_1+\omega_2))], \\
g_4(s) &= \mathcal{C}_1(0)(s+i\omega_2)(s+i\omega_3) - \mathcal{F}_1(s) \\
&\quad \times [\mathcal{C}_3(0)(s+i\omega_2) + \mathcal{C}_2(0)(s+i\omega_3) - \mathcal{C}_1(0) \\
&\quad \times (2s + i(\omega_2+\omega_3))], \\
g_5(s) &= \mathcal{C}_2(0)(s+i\omega_1)(s+i\omega_3) - \mathcal{F}_1(s) \\
&\quad \times [\mathcal{C}_3(0)(s+i\omega_1) + \mathcal{C}_1(0)(s+i\omega_3) - \mathcal{C}_2(0) \\
&\quad \times (2s + i(\omega_1+\omega_3))], \\
g_6(s) &= \mathcal{C}_3(0)(s+i\omega_1)(s+i\omega_2) - \mathcal{F}_1(s) \\
&\quad \times [\mathcal{C}_2(0)(s+i\omega_1) + \mathcal{C}_1(0)(s+i\omega_2) - \mathcal{C}_3(0) \\
&\quad \times (2s + i(\omega_1+\omega_2))], \\
\nu_1(s) &= g_4(s)/\mathcal{L}_3(s) - g_1(s)/\mathcal{G}_3(s), \\
\nu_2(s) &= g_5(s)/\mathcal{L}_3(s) - g_2(s)/\mathcal{G}_3(s), \\
\nu_3(s) &= g_6(s)/\mathcal{L}_3(s) - g_3(s)/\mathcal{G}_3(s).
\end{aligned}$$

For N nonidentical atoms with different transition frequencies ($N > 3$, $\omega_1 \neq \omega_2 \neq \cdots \neq \omega_N$), following the similar methods as above, we also can obtain the exact non-Markovian dynamics under the single excitation space. In this paper, we are not going to have further discussions about it.

[1] H. P. Breuer and F. Petruccione, *The Theory of Open Quantum Systems* (Oxford University Press, Oxford, UK, 2002).

[2] C. W. Gardiner and P. Zoller, *Quantum Noise* (Springer, Berlin, 2004).

[3] D. P. DiVincenzo, Quantum computation, Science **270**, 255 (1995).

[4] M. A. Nielsen and I. L. Chuang, *Quantum Computation and Quantum Information* (Cambridge University Press, Cambridge, UK, 2000).

[5] S. L. Su, H. Z. Shen, E. J. Liang, and S. Zhang, One-step construction of the multiple-qubit Rydberg controlled-phase gate, Phys. Rev. A **98**, 032306 (2018); S. L. Su, Y. Z. Tian, H. Z. Shen, H. P. Zang, E. J. Liang, and S. Zhang, Applications of the modified Rydberg antiblockade regime with simultaneous driving, *ibid.* **96**, 042335 (2017); S. L. Su, Y. Gao, E. J. Liang, and S. Zhang, Fast Rydberg antiblockade regime and its applications in quantum logic gates, *ibid.* **95**, 022319 (2017).

[6] H. P. Breuer, E. M. Laine, J. Piilo, and B. Vacchini, *Colloquium*: Non-Markovian dynamics in open quantum systems, Rev. Mod. Phys. **88**, 021002 (2016).

[7] I. de Vega and D. Alonso, Dynamics of non-Markovian open quantum systems, Rev. Mod. Phys. **89**, 015001 (2017).

[8] L. Chirolli and G. Burkard, Decoherence in solid-state qubits, Adv. Phys. **57**, 225 (2008).

[9] G. Burkard, Non-Markovian qubit dynamics in the presence of $1/f$ noise, Phys. Rev. B **79**, 125317 (2009).

[10] H. T. Tan and W. M. Zhang, Non-Markovian dynamics of an open quantum system with initial system-reservoir correlations: A nanocavity coupled to a coupled-resonator optical waveguide, Phys. Rev. A **83**, 032102 (2011).

[11] M. W. Y. Tu and W. M. Zhang, Non-Markovian decoherence theory for a double-dot charge qubit, Phys. Rev. B **78**, 235311 (2008).

[12] J. S. Jin, M. W. Y. Tu, W. M. Zhang, and Y. J. Yan, Non-equilibrium quantum theory for nanodevices based on the Feynman-Vernon influence functional, New J. Phys. **12**, 083013 (2010).

[13] C. J. Myatt, B. E. King, Q. A. Turchette, C. A. Sackett, D. Kielpinski, W. M. Itano, C. Monroe, and D. J. Wineland, Decoherence of quantum superpositions through coupling to engineered reservoirs, Nature (London) **403**, 269 (2000).

[14] M. Notomi, Manipulating light with strongly modulated photonic crystals, Rep. Prog. Phys. **73**, 096501 (2010).

[15] C. Luo, M. Ibanescu, S. G. Johnson, and J. D. Joannopoulos, Cerenkov radiation in photonic crystals, Science **299**, 368 (2003).

[16] C. Luo, M. Ibanescu, E. J. Reed, S. G. Johnson, and J. D. Joannopoulos, Doppler Radiation Emitted by an Oscillating Dipole Moving Inside a Photonic Band-Gap Crystal, Phys. Rev. Lett. **96**, 043903 (2006).

[17] D. E. Chang, L. Jiang, A. V. Gorshkov, and H. J. Kimble, Cavity QED with atomic mirrors, New J. Phys. **14**, 063003 (2012).

[18] A. González-Tudela and D. Porras, Mesoscopic Entanglement Induced by Spontaneous Emission in Solid-State Quantum Optics, Phys. Rev. Lett. **110**, 080502 (2013).

[19] H. Z. Shen, M. Qin, and X. X. Yi, Single-photon storing in coupled non-Markovian atom-cavity system, Phys. Rev. A **88**, 033835 (2013); H. Z. Shen, M. Qin, X. Q. Shao, and X. X. Yi, General response formula and application to topological insulator in quantum open system, Phys. Rev. E **92**, 052122 (2015); H. Z. Shen, D. X. Li, and X. X. Yi, Non-Markovian linear response theory for quantum open systems and its applications, *ibid.* **95**, 012156 (2017).

[20] S. B. Xue, R. B. Wu, W. M. Zhang, J. Zhang, C. W. Li, and T. J. Tarn, Decoherence suppression via non-Markovian coherent feedback control, Phys. Rev. A **86**, 052304 (2012).

[21] J. Zhang, Y. X. Liu, R. B. Wu, K. Jacobs, and F. Nori, Quantum feedback: Theory, experiments, and applications, Phys. Rep. **679**, 1 (2017).

[22] J. Combes, J. Kerckhoff, and M. Sarovar, The SLH framework for modeling quantum input-output networks, Adv. Phys. X **2**, 784 (2017).

[23] L. Viola and S. Lloyd, Dynamical suppression of decoherence in two-state quantum systems, Phys. Rev. A **58**, 2733 (1998).

[24] L. Viola, E. Knill, and S. Lloyd, Dynamical Decoupling of Open Quantum Systems, Phys. Rev. Lett. **82**, 2417 (1999).

[25] L. A. Wu, M. S. Byrd, and D. A. Lidar, Efficient Universal Leakage Elimination for Physical and Encoded Qubits, Phys. Rev. Lett. **89**, 127901 (2002).

[26] A. G. Kofman and G. Kurizki, Unified Theory of Dynamically Suppressed Qubit Decoherence in Thermal Baths, Phys. Rev. Lett. **93**, 130406 (2004).

[27] G. S. Uhrig, Exact results on dynamical decoupling by π pulses in quantum information processes, New J. Phys. **10**, 083024 (2008).

[28] G. S. Uhrig, Concatenated Control Sequences Based on Optimized Dynamic Decoupling, Phys. Rev. Lett. **102**, 120502 (2009).

[29] Y. Pan, Z. R. Xi, and J. Gong, Optimized dynamical decoupling sequences in protecting two-qubit states, J. Phys. B **44**, 175501 (2011).

[30] A. Z. Chaudhry and J. Gong, Decoherence control: Universal protection of two-qubit states and two-qubit gates using continuous driving fields, Phys. Rev. A **85**, 012315 (2012).

[31] W. Shu, X. Zhao, J. Jing, L. A. Wu, and T. Yu, Uhrig dynamical control of a three-level system via non-Markovian quantum state diffusion, J. Phys. B **46**, 175504 (2013).

[32] J. Jing, T. Yu, C. H. Lam, J. Q. You, and L. A. Wu, Control relaxation via dephasing: A quantum-state-diffusion study, Phys. Rev. A **97**, 012104 (2018).

[33] S. John and J. Wang, Quantum Electrodynamics near a Photonic Band Gap: Photon Bound States and Dressed Atoms, Phys. Rev. Lett. **64**, 2418 (1990).

[34] E. Yablonovitch, Inhibited Spontaneous Emission in Solid-State Physics and Electronics, Phys. Rev. Lett. **58**, 2059 (1987).

[35] A. G. Kofman, G. Kurizki, and B. Sherman, Spontaneous and induced atomic decay in photonic band structures, J. Mod. Opt. **41**, 353 (1994).

[36] Y. Liu and A. A. Houck, Quantum electrodynamics near a photonic bandgap, Nat. Phys. **13**, 48 (2017).

[37] S. Noda, M. Fujita, and T. Asano, Spontaneous-emission control by photonic crystals and nanocavities, Nat. Photon. **1**, 449 (2007).

[38] P. Lodahl, A. F. Van Driel, I. S. Nikolaev, A. Irman, K. Overgaag, D. Vanmaekelbergh, and W. L. Vos, Controlling the dynamics of spontaneous emission from quantum dots by photonic crystals, Nature (London) **430**, 654 (2004).

[39] H. B. Liu, J. H. An, C. Chen, Q. J. Tong, H. G. Luo, and C. H. Oh, Anomalous decoherence in a dissipative two-level system, Phys. Rev. A **87**, 052139 (2013).

[40] H. B. Liu, W. L. Yang, J. H. An, and Z. Y. Xu, Mechanism for quantum speedup in open quantum systems, Phys. Rev. A **93**, 020105(R) (2016).

[41] P. Zhang, B. You, and L. X. Cen, Long-lived quantum coherence of two-level spontaneous emission models within structured environments, Opt. Lett. **38**, 3650 (2013).

[42] T. Ramos, B. Vermersch, P. Hauke, H. Pichler, and P. Zoller, Non-Markovian dynamics in chiral quantum networks with spins and photons, Phys. Rev. A **93**, 062104 (2016).

[43] N. Behzadi, B. Ahansaz, A. Ektesabi, and E. Faizi, Controlling speedup in open quantum systems through manipulation of system-reservoir bound states, Phys. Rev. A **95**, 052121 (2017).

[44] H. T. Cui, H. Z. Shen, S. C. Hou, and X. X. Yi, Bound state and localization of excitation in many-body open systems, Phys. Rev. A **97**, 042129 (2018).

[45] P. Facchi, M. S. Kim, S. Pascazio, F. V. Pepe, D. Pomarico, and T. Tufarelli, Bound states and entanglement generation in waveguide quantum electrodynamics, Phys. Rev. A **94**, 043839 (2016).

[46] A. González-Tudela and J. I. Cirac, Exotic quantum dynamics and purely long-range coherent interactions in Dirac conelike baths, Phys. Rev. A **97**, 043831 (2018).

[47] C. Ma, Y. S. Wang, and J. H. An, Floquet engineering of localized propagation of light in a waveguide array, Phys. Rev. A **97**, 023808 (2018).

[48] C. J. Yang and J. H. An, Suppressed dissipation of a quantum emitter coupled to surface plasmon polaritons, Phys. Rev. B **95**, 161408(R) (2017).

[49] H. Z. Shen, X. Q. Shao, G. C. Wang, X. L. Zhao, and X. X. Yi, Quantum phase transition in a coupled two-level system embedded in anisotropic three-dimensional photonic crystals, Phys. Rev. E **93**, 012107 (2016).

[50] C. D. Parmee and N. R. Cooper, Decay rates and energies of free magnons and bound states in dissipative XXZ chains, arXiv:1812.07893.

[51] H. Z. Shen, S. Xu, S. Yi, and X. X. Yi, Controllable dissipation of a qubit coupled to an engineering reservoir, Phys. Rev. A **98**, 062106 (2018); H. Z. Shen, H. Li, Y. F. Peng, and X. X. Yi, Mechanism for Hall conductance of two-band systems against decoherence, Phys. Rev. E **95**, 042129 (2017).

[52] P. Facchi, S. Pascazio, F. V. Pepe, and D. Pomarico, Correlated photon emission by two excited atoms in a waveguide, Phys. Rev. A **98**, 063823 (2018).

[53] C. Y. Cai, L. P. Yang, and C. P. Sun, Threshold for nonthermal stabilization of open quantum systems, Phys. Rev. A **89**, 012128 (2014).

[54] H. J. Zhu, G. F. Zhang, L. Zhuang, and W. M. Liu, Universal Dissipationless Dynamics in Gaussian Continuous-Variable Open Systems, Phys. Rev. Lett. **121**, 220403 (2018).

[55] C. W. Hsu, B. Zhen, A. D. Stone, J. D. Joannopoulos, and M. Soljačić, Bound states in the continuum, Nat. Rev. Mater. **1**, 16048 (2016).

[56] P. T. Fong and C. K. Law, Bound state in the continuum by spatially separated ensembles of atoms in a coupled-cavity array, Phys. Rev. A **96**, 023842 (2017).

[57] Y. V. Kartashov, V. V. Konotop, and L. Torner, Bound states in the continuum in spin-orbit-coupled atomic systems, Phys. Rev. A **96**, 033619 (2017).

[58] G. Della Valle and S. Longhi, Floquet-Hubbard bound states in the continuum, Phys. Rev. B **89**, 115118 (2014).
[59] S. Longhi and G. Della Valle, Floquet bound states in the continuum, Sci. Rep. **3**, 2219 (2013).
[60] G. Calajó, Y.-L. L. Fang, H. U. Baranger, and F. Ciccarello, Exciting a Bound State in the Continuum through Multi-Photon Scattering plus Delayed Quantum Feedback, Phys. Rev. Lett. **122**, 073601 (2019).
[61] S. Garmon, K. Noba, G. Ordonez, and D. Segal, Non-Markovian dynamics revealed at the bound state in continuum, Phys. Rev. A **99**, 010102 (2019).
[62] A. González-Tudela and J. I. Cirac, Markovian and non-Markovian dynamics of quantum emitters coupled to two-dimensional structured reservoirs, Phys. Rev. A **96**, 043811 (2017).
[63] A. González-Tudela and J. I. Cirac, Quantum Emitters in Two-Dimensional Structured Reservoirs in the Nonperturbative Regime, Phys. Rev. Lett. **119**, 143602 (2017).
[64] F. Galve and R. Zambrini, Coherent and radiative couplings through two-dimensional structured environments, Phys. Rev. A **97**, 033846 (2018).
[65] A. González-Tudela and J. I. Cirac, Non-Markovian quantum optics with three-dimensional state-dependent optical lattices, Quantum **2**, 97 (2018).
[66] I. de Vega, D. Porras, and J. I. Cirac, Matter-Wave Emission in Optical Lattices: Single Particle and Collective Effects, Phys. Rev. Lett. **101**, 260404 (2008).
[67] G. Calajó, F. Ciccarello, D. Chang, and P. Rabl, Atom-field dressed states in slow-light waveguide QED, Phys. Rev. A **93**, 033833 (2016).
[68] T. Shi, Y. H. Wu, A. González-Tudela, and J. I. Cirac, Bound States in Boson Impurity Models, Phys. Rev. X **6**, 021027 (2016).
[69] T. Shi, Y. H Wu, A. González-Tudela and J. I. Cirac, Effective many-body Hamiltonians of qubit-photon bound states, New J. Phys. **20**, 105005 (2018).
[70] E. Sánchez-Burillo, D. Zueco, L. Martin-Moreno, and J. J. García-Ripoll, Dynamical signatures of bound states in waveguide QED, Phys. Rev. A **96**, 023831 (2017).
[71] G. Calajó and P. Rabl, Strong coupling between moving atoms and slow-light Cherenkov photons, Phys. Rev. A **95**, 043824 (2017).
[72] M. Stewart, L. Krinner, A. Pazmiño, and D. Schneble, Analysis of non-Markovian coupling of a lattice-trapped atom to free space, Phys. Rev. A **95**, 013626 (2017).
[73] L. Krinner, M. Stewart, A. Pazmiño, J. Kwon, and D. Schneble, Spontaneous Emission in a Matter-Wave Open Quantum System, Nature **559**, 589 (2018).
[74] N. M Sundaresan, R. Lundgren, G. Y. Zhu, A. V. Gorshkov, and A. A. Houck, Interacting Qubit-Photon Bound States with Superconducting Circuits, Phys. Rev. X **9**, 011021 (2019).
[75] S. John, Strong Localization of Photons in Certain Disordered Dielectric Superlattices, Phys. Rev. Lett. **58**, 2486 (1987).
[76] P. Ullersma, An exactly solvable model for Brownian motion: I. Derivation of the Langevin equation, Physica **32**, 27 (1966).
[77] P. Ullersma, An exactly solvable model for Brownian motion: II. Derivation of the Fokker-Planck equation and the master equation, Physica **32**, 56 (1966).
[78] P. Ullersma, An exactly solvable model for Brownian motion: III. Motion of a heavy mass in a linear chain, Physica **32**, 74 (1966).
[79] P. Ullersma, An exactly solvable model for Brownian motion: IV. Susceptibility and Nyquist's theorem, Physica **32**, 90 (1966).
[80] S. John and T. Quang, Spontaneous emission near the edge of a photonic band gap, Phys. Rev. A **50**, 1764 (1994).
[81] L. Ortiz-Gutiérrez, L. F. Muñoz-Martínez, D. F. Barros, J. E. O. Morales, R. S. N. Moreira, N. D. Alves, A. F. G. Tieco, P. L. Saldanha, and D. Felinto, Experimental Fock-State Superradiance, Phys. Rev. Lett. **120**, 083603 (2018).
[82] M. Hebenstreit, B. Kraus, L. Ostermann, and H. Ritsch, Subradiance via Entanglement in Atoms with Several Independent Decay Channels, Phys. Rev. Lett. **118**, 143602 (2017).
[83] N. Cui, M. Macovei, K. Z. Hatsagortsyan, and C. H. Keitel, Manipulating the Annihilation Dynamics of Positronium via Collective Radiation, Phys. Rev. Lett. **108**, 243401 (2012).
[84] M. Nagasono, J. R. Harries, H. Iwayama, T. Togashi, K. Tono, M. Yabashi, Y. Senba, H. Ohashi, T. Ishikawa, and E. Shigemasa, Observation of Free-Electron-Laser-Induced Collective Spontaneous Emission (Superfluorescence), Phys. Rev. Lett. **107**, 193603 (2011).
[85] S. Mokhlespour, J. E. M. Haverkort, G. Slepyan, S. Maksimenko, and A. Hoffmann, Collective spontaneous emission in coupled quantum dots: Physical mechanism of quantum nanoantenna, Phys. Rev. B **86**, 245322 (2012).
[86] A. A. Svidzinsky, J. T. Chang, and M. O. Scully, Dynamical Evolution of Correlated Spontaneous Emission of a Single Photon from a Uniformly Excited Cloud of N Atoms, Phys. Rev. Lett. **100**, 160504 (2008).
[87] A. A. Svidzinsky, J. T. Chang, and M. O. Scully, Cooperative spontaneous emission of N atoms: Many-body eigenstates, the effect of virtual Lamb shift processes, and analogy with radiation of N classical oscillators, Phys. Rev. A **81**, 053821 (2010).
[88] J. P. Clemens, L. Horvath, B. C. Sanders, and H. J. Carmichael, Collective spontaneous emission from a line of atoms, Phys. Rev. A **68**, 023809 (2003).
[89] S. Bochner and K. Chandrasekharan, *Fourier Transforms* (Princeton University Press, Princeton, NJ, 1949).
[90] P. Lambropoulos, G. M. Nikolopoulos, T. R. Nielsen, and S. Bay, Fundamental quantum optics in structured reservoir, Rep. Prog. Phys. **63**, 455 (2000).
[91] S. Bay, P. Lambropoulos, and K. Mølmer, Atom-atom interaction in strongly modified reservoirs, Phys. Rev. A **55**, 1485 (1997).
[92] S. Bay, P. Lambropoulos, and K. Mølmer, Superradiance in a structured radiation reservoir, Phys. Rev. A **57**, 3065 (1998).
[93] S. John and T. Quang, Localization of Superradiance near a Photonic Band Gap, Phys. Rev. Lett. **74**, 3419 (1995).
[94] W. K. Wootters, Entanglement of Formation of an Arbitrary State of Two Qubits, Phys. Rev. Lett. **80**, 2245 (1998); T. Yu and J. H. Eberly, Finite-Time Disentanglement via Spontaneous Emission, *ibid.* **93**, 140404 (2004).
[95] N. Vats and S. John, Non-Markovian quantum fluctuations and superradiance near a photonic band edge, Phys. Rev. A **58**, 4168 (1998).
[96] N. Vats, S. John, and K. Busch, Theory of fluorescence in photonic crystals, Phys. Rev. A **65**, 043808 (2002).

[97] W. H. Louisell, *Quantum Statistical Properties of Radiation* (John Wiley and Sons, Inc., New York, 1973).

[98] H. Z. Shen, C. Shang, Y. H. Zhou, and X. X. Yi, Unconventional single-photon blockade in non-Markovian systems, Phys. Rev. A **98**, 023856 (2018); H. Z. Shen, S. L. Su, Y. H. Zhou, and X. X. Yi, Non-Markovian quantum Brownian motion in one dimension in electric fields, *ibid.* **97**, 042121 (2018); H. Z. Shen, D. X. Li, S. L. Su, Y. H. Zhou, and X. X. Yi, Exact non-Markovian dynamics of qubits coupled to two interacting environments, *ibid.* **96**, 033805 (2017).

[99] S. Gröblacher, A. Trubarov, N. Prigge, G. D. Cole, M. Aspelmeyer, and J. Eisert, Observation of non-Markovian micromechanical Brownian motion, Nat. Commun. **6**, 7606 (2015).

[100] Z. Ficek and S. Swain, Simulating quantum interference in a three-level system with perpendicular transition dipole moments, Phys. Rev. A **69**, 023401 (2004).

[101] J. Evers and C. H. Keitel, Spontaneous-Emission Suppression on Arbitrary Atomic Transitions, Phys. Rev. Lett. **89**, 163601 (2002).